AN EXPERIMENTAL STUDY ON DESIGN AND CHARACTERIZATION OF CO_2 ADSORBENTS

by

Burcu Acar

B.S., Chemical Engineering, Boğaziçi University, 2012

Submitted to the Institute for Graduate Studies in
Science and Engineering in partial fulfillment of
the requirements for the degree of
Master of Science

Graduate Program in Chemical Engineering
Boğaziçi University

2016

AN EXPERIMENTAL STUDY ON DESIGN AND CHARACTERIZATION OF CO_2 ADSORBENTS

APPROVED BY:

Prof. Ahmet Erhan Aksoylu (Thesis Supervisor)	...…….
Prof. Ramazan Yıldırım	…….
Assoc. Prof. Hasan Bedir	...…….

DATE OF APPROVAL: 11.01.2016

to my family

ACKNOWLEDGEMENTS

Firstly, I would like to express my sincere gratitude to my thesis supervisor Prof. Ahmet Erhan Aksoylu for his guidance, immense knowledge, support, and trust in me. His guidance helped me in all the time of research and writing of this thesis. It was a privilege for me to work with him during my study.

My sincere thanks also go to Burcu Selen Çağlayan not only for her expertise in adsorption modelling and kinetic studies, but also for her encouragement, guidance and for enlightening me by giving her practical advices whenever I needed throughout my work.

I would like to express my sincere appreciations for the members of my thesis committee, Prof. Ramazan Yıldırım and Assoc. Prof. Hasan Bedir, for devoting their valuable time to attend my thesis defense.

I am deeply grateful to two special people, my friends Melek Selcen Başar and Merve Eropak for guiding and helping me throughout my thesis. I would never succeed without them.

I would like to thank to Emre Demirel, Doğa Demirhan, Elif Erdinç, Serhat Erşahin, Manouchehr Nadjafi, Çağla Odabaşı, İpek Paksoy, Özgü Özer, Ali Uzun and all CATREL team members in the Chemical Engineering Department at Boğaziçi University for their friendship and making this period enjoyable.

I should also thank to Bilge Gedik Uluocak for her significant effort in SEM analyses conducted at Boğaziçi University Advanced Technologies Research and Development Center.

Very special thanks should be addressed to Serli Kiremitçiyan, Elif Tezel and Yasemin Yeşiltepe for their friendship, endless support and encouragement on any matter.

Finally, I wish to express the profound gratitude to my beloved family, my father Mustafa Acar, my mother Ayfer Acar, and my sister Kübra Acar. Although my father passed away years ago, I continue to feel his trust and love in me. My amazing family to whom this dissertation is dedicated to, has always believed in me and gave me love, strength and courage to follow my dreams and desires.

Financial support for this study provided by TÜBİTAK through project 113M263 is gratefully acknowledged.

ABSTRACT

AN EXPERIMENTAL STUDY ON DESIGN AND CHARACTERIZATION OF CO_2 ADSORBENTS

The aim of this study is to design and develop AC-based CO_2 adsorbent(s) having both high and stable CO_2 adsorption capacity, and ability to adsorb CO_2 selectively from CO_2-CH_4 mixture. In this context, a commercial activated carbon, Norit ROX, was oxidized by air and HNO_3 oxidation, and two series of adsorbents, AC8 and AC9 series, respectively, were prepared on those oxidized ACs by K_2CO_3 impregnation following by calcination at various temperatures. The adsorbent samples were characterized by SEM-EDX for analyzing their microstructural properties and alkali dispersion on their surface. The clusters formed on AC8 adsorbents were not homogeneously distributed over the adsorbent, whereas AC9 adsorbents had homogeneously dispersed K-formations on their surfaces. Adsorption/desorption and selective adsorption tests were conducted for 0-1000 mbar pressure range under 50 ml/min gas flow rate at room temperature (RT), 120 °C and 200 °C for pure CO_2, pure CH_4 and their mixtures, 50% CO_2-50% CH_4 and 10% CO_2-90% CH_4. The adsorption/selective adsorption performance of AC9 series, were inferior to the performance of the AC8 series adsorbents. The highest CO_2 adsorption capacity, ca. 11 wt.%, was observed for AC8-300 sample at RT. CO_2 adsorption was confirmed to be reversible, whereas CH_4 adsorption was partially irreversible. Although AC8-200 has the highest mass based CO_2:CH_4 adsorption selectivity ratio, ca. 3.7, at RT for the 50% CO_2-50% CH_4 mixture, for the 10% CO_2-90% CH_4 mixture, mass based adsorption selectivity ratio was at its highest on AC8-250 with a value of 0.59. AC8-200 was further tested for 0-5000 mbar pressure range at RT under 50 ml/min pure CO_2 and pure CH_4 flow and 90 ml/min total flow of 50% CO_2-50% CH_4 and 10% CO_2-90% CH_4 gas mixtures. The CO_2 adsorption capacity was measured as 19.7 wt.% at 5000 mbar. The experimental adsorption isotherm data were fitted to Langmuir, Freundlich and Dubinin-Radushkevich (D-R) models. D-R model was the most successful in explaining CO_2 and CH_4 adsorption behaviors of AC samples. Between the kinetic models, pseudo-first order kinetic model successfully explained both CO_2 and CH_4 adsorption kinetics at RT, whereas CH_4 adsorption kinetics on AC8-200 and AC8-300 were more suitably explained by pseudo-second order kinetic model.

ÖZET

KARBON DİOKSİT ADSORBANLARININ TASARIMI VE GELİŞTİRİLMESİ ÜZERİNE DENEYSEL ÇALIŞMA

Bu çalışmanın amacı, yüksek ve kararlı adsorpsiyon kapasitesine ve CO_2-CH_4 karışımı içinden seçimli CO_2 adsorpsiyonu yapabilme yeteneğine sahip aktif karbon (AC) bazlı karbon dioksit adsorbanlarının tasarımı ve geliştirilmesidir. Bu bağlamda, ticari bir AC, Norit ROX, hava ve HNO_3 ile okside edilerek sırasıyla AC8 ve AC9 adsorban setleri bu okside edilmiş AC'lerin üzerine farklı sıcaklıklarda kalsinasyonu yapılan K_2CO_3 empregnasyonuyla hazırlanmıştır. Adsorban örnekleri mikro-yapısal özelliklerinin ve yüzeylerindeki alkali dağılımının analiz edilmesi için SEM-EDX'le karakterize edilmiştir. AC8 adsorbanlarının yüzeyindeki K^+ kümelenmeleri homojen dağılmazken, AC9 adsorbanlarının yüzeylerinde K-oluşumları homojen dağılmıştır. Adsorpsiyon/desorpsiyon ve seçimli adsorpsiyon testleri, 0-1000 mbar basınç aralığında, 50 ml/dak toplam gaz akışı altında, oda sıcaklığında, 120 °C ve 200 °C'de, saf CO_2, saf CH_4 ve bu iki gazın karışımları, %50 CO_2-%50 CH_4 ve %10CO_2-%90 CH_4, için yapılmıştır. AC8 adsorban seti, AC9 adsorban setinden daha yüksek adsorpsiyon/seçimli adsorpsiyon performansı göstermiştir. En yüksek CO_2 adsorpsiyonu kütlece %11 ile AC8-300 örneği üzerinde oda sıcaklığında gözlenmiştir. CO_2 adsorpsiyonunun tersinir, CH_4 adsorpsiyonunun ise kısmen tersinmez olduğu tespit edilmiştir. Oda sıcaklığında, %50 CO_2-%50 CH_4 karışımı için AC8-200, 3.7 ile kütlece en yüksek CO_2:CH_4 adsorpsiyon seçimliliğine sahipken, %10 CO_2-%90 CH_4 karışımı için en yüksek adsorpsiyon seçimlilik oranı 0.59 ile AC8-250'de gözlenmiştir. AC8-200 adsorbanı 0-5000 mbar basınç aralığı için, oda sıcaklığında, 50 ml/dak saf CO_2 ve saf CH_4 akışı altında ve %50 CO_2-%50 CH_4 ve %10 CO_2-%90 CH_4 gaz karışımları için toplam 90 ml/dak gaz akışı altında test edilmiştir. 5000 mbar'da CO_2 adsorpsiyon kapasitesi kütlece %19 olarak ölçülmüştür. Deneysel adsorpsiyon izotermlerinin Langmuir, Freundlich ve Dubinin-Radushkevich (D-R) modellerine uygunluğu araştırılmıştır. AC örneklerinin CO_2 ve CH_4 adsorpsiyon davranışını açıklamaya en uygun modelin D-R modeli olduğu saptanmıştır. Hem CO_2 hem de CH_4 adsorpsiyon kinetiği oda sıcaklığında psödo-birinci derece kinetik model ile açıklanabiliyorken, AC8-200 ve AC8-300 adsorbanlarının üzerinde CH_4 adsorpsiyon kinetiği psödo-ikinci derece kinetik denkleme uygunluk göstermektedir.

TABLE OF CONTENTS

LIST OF FIGURES

LIST OF TABLES

LIST OF SYMBOLS

CH_4	Methane
CO_2	Carbon dioxide
E	The characteristic energy of the system
H_2	Hydrogen
H_2O	Water
HCl	Hydrochloric acid
HNO_3	Nitric acid
K	Potassium
KOH	Potassium hydroxide
L	Liter
min	Minute
mL	Milliliter
n	Adsorbent heterogeneity parameter
N_2	Nitrogen
N_2O	Nitrous oxide
O_2	Oxygen
P	Pressure
R	Universal gas constant
S	Surface area
t	Adsorbent heterogeneity parameter
T	Temperature

LIST OF ACRONYMS/ABBREVIATIONS

AC	Active Carbon
AC1	HCl Treated Activated Carbon
AC2	Air Oxidized Activated Carbon
AC3	Nitric Acid Oxidized Activated Carbon
AC8	Air Oxidized and K_2CO_3 Impregnated Activated Carbon
AC9	HNO_3 Oxidized and K_2CO_3 Impregnated Activated Carbon
AlPO	Alumino-Phosphates
BET	Brunauer-Emmett-Teller
BOS	Birleşik Oksijen Sanayi
BSE	Back-Scattering Electron
CCS	Carbon Capture and Sequestration
CFC	Chlorofluorocarbons
CMS	Carbon Molecular Sieves
CNT	Carbon Nanotubes
DSMS	Dynamic Sampling Mass Spectrometer
EDX	Energy Dispersive X-Ray Spectroscopy
FTIR	Fourier Transform Infrared
IGA	Intelligent Gravimetric Analyzer
LNG	Liquefied Natural Gas
MBS	Molecular Basket Sorbents
MEA	Monoethanol Amine
MOF	Metal Organic Frameworks
NG	Natural Gas
PEI	Polyethylenimine
SAPO	Alumino-Silico-Phosphates
SE	Secondary Electron
SEM	Scanning Electron Microscopy
WGS	Water-Gas Shift
XPS	X-Ray Photoelectron Spectroscopy

1. INTRODUCTION

Accumulation of greenhouse gases in the atmosphere is responsible for air pollution and various environmental problems, like global climate change, continuous rise of water-level in sea, the increasing number of ocean storms, floods, etc. [1].

Atmospheric greenhouse gas concentration is increasing mainly as a result of combustion of fossil fuels, deforestation and desertification. Carbon dioxide (CO_2), methane (CH_4), chlorofluorocarbons (CFCs), and nitrous oxide (N_2O) are the primary greenhouse gases [2]. Carbon dioxide is the fourth most abundant gas in the atmosphere. Although it is naturally present in the atmosphere, its concentration is rising [3].

85% of the total energy requirement of the world is supplied by fossil fuel based power production plants (coal, oil, gas), and nearly 40% of CO_2 in the atmosphere is emitted by these fossil fuel plants. In abatement of CO_2 emission to the atmosphere originating from these units, carbon capture and sequestration technologies have a high potential. As CCS currently is an expensive process, costing roughly 40% of the total cost of power plant, cost effective CCS options need to be developed and proliferated [4-6].

Depending on the plant technology and configuration, CO_2 emissions from a power plant flue gas can be reduced by any of the following methods [4, 7]:

- Pre-combustion capture
- Post-combustion capture
- Oxyfuel combustion

In pre-combustion capture systems, in general, the primary fossil fuel is first reformed by oxygen and/or steam, and then effluent is sent to a water-gas shift (WGS) unit. The WGS product is a hydrogen rich stream having CO_2. The CO_2 then can be separated from H_2, and the pure hydrogen is combusted with air in the power plant. The separation of CO_2 and H_2 can be done by absorption, adsorption or membranes [4-5].

Post-combustion capture is the capture of CO_2 in the exhaust gas once the fuel has been fully combusted. Power plants generate flue gas with low CO_2 concentration, less than 15%, due to high N_2 content of air used in combustion. As CO_2 concentration is low, the thermodynamic driving force of capture is weak, creating a technical challenge for the development of advanced capture processes. Currently chemical absorption technologies appear best adapted to this capture method [4, 7].

For oxy-fuel combustion, the combustion process is performed with pure oxygen, which is produced from air by using cryogenic or membrane separation. The combustion products are essentially CO_2 and H_2O, which are separated by condensing water. The combustion with pure oxygen leads to high temperatures when compared with the combustion with air. The recycle of CO_2-rich flue gas reduces the temperature to usual values. The stream with high concentrations of CO_2 is sent to the capture unit [4-5].

Absorption, membrane and cryogenic separation, and adsorption are the available technologies which are employed in the CO_2-capture step of the above mentioned methods [4].

Absorption is the most commonly used method based on the reaction between CO_2 and a chemical solvent, such as aqueous solution of mono-, di- and tri-amine, di-isopropanol amine, etc. During CO_2 capture, the absorbent is introduced to flue gas stream containing CO_2, and the selective absorption of CO_2 occurs. In the regeneration step, CO_2 is desorbed, then the regenerated solvent is recycled for further use, while desorbed CO_2 is compressed and sent to storage. The most important problem associated with absorption is the high amount of energy required for regeneration step [4].

Cryogenic distillation is an air separation process, where gaseous components are separated by condensation. Cryogenic method can capture CO_2 in liquid form, which is easier to transport and store or to send for enhanced oil recovery fields. However, it is not used for dilute CO_2 streams as the amount of energy required is uneconomical [4-5].

Membrane process operates on the principle of preferential permeation of mixture constituents through the pores of the membrane. Various types of gas separation membranes including ceramic, polymeric and combination of both materials are available [4].

Adsorption is an alternative method to separate compounds from the industrial gas mixtures. The separation is achieved when a certain component (called adsorbate) in a mixture attaches to the surface of a solid (called adsorbent) whereas the others remain in the gas stream. As adsorption is an exothermic process, unlike what is experienced in absorption, the regeneration step of adsorbents does not need high energy input. Additionally, the adsorbents can be used for wide ranges of CO_2 concentrations and process temperatures. Due to the above mentioned advantages, adsorption has a potential to be widely used in carbon capturing processes in the future. The most important requirement for the wide use of this technique is the development of adsorbents having high selectivity and good adsorption capacity for the target gas component, fast adsorption and desorption kinetics, good physical and chemical stability through adsorption/desorption cycles and be regenerable by modest pressure and temperature swings to minimize operational energy costs [8-9].

The purpose of the current study is to design and develop AC-based CO_2 adsorbent(s) having both high and stable CO_2 adsorption capacity, and ability to adsorb CO_2 selectively from CO_2-CH_4 mixture. In this context, a commercial activated carbon, Norit ROX, was oxidized by air and HNO_3 oxidation, and two series of adsorbents, AC8 and AC9 series, respectively, were prepared on those oxidized ACs by K_2CO_3 impregnation following by calcination at various temperatures. The adsorbent samples were characterized by SEM-EDX for analyzing their microstructural properties and alkali dispersion on their surface and tested by IGA-DSMS system for their adsorption/selective adsorption performances.

2. LITERATURE SURVEY

2.1. Adsorption

Adsorption is taught as one of the most promising approach due to the low energy requirement owing to exothermicity of the process, cost advantage, and ease of applicability over a relatively wide range of temperatures and pressures. The most important requirement for the wide use of this technique is the development of adsorbents having high selectivity and good adsorption capacity for the target gas component, fast adsorption and desorption kinetics, good physical and chemical stability through adsorption/desorption cycles and be regenerable by modest pressure or temperature swings to minimize operational energy costs [8-9].

The use of appropriate adsorbents for CO_2 capture has a potential in reducing the cost of CO_2 separation in the overall carbon capture and storage (CCS) process. In order to design and develop the most appropriate adsorbent(s), many materials are produced, characterized and tested for their selectivity and adsorption properties.

Adsorbents for CO_2 capture can be categorized in many ways, based on their chemical composition, structural characteristics or according to the adsorption mechanism involved, i.e., physical or chemical. The CO_2 chemical adsorbents refer to those obtained through incorporation of amine groups into solid supports such as mesoporous silica [10].

Absorption with liquid amine solutions is the technology used in industry for CO_2 capture. The liquid amine absorption process inspired researchers to use amine-modified solid materials as adsorbents for CO_2 capture. It was assumed that supported amines will show a high selectivity for CO_2 over other flue gas components, particularly N_2. The early efforts to produce amine functionalized adsorbents were not successful in terms of adsorption capacity. On the other hand, the studies resulted in significant performance improvements, leading to increasing interest for this matter. The type of interactions between amine groups and the support may be used for categorization; amine-impregnated and

amine-grafted materials via weak interactions and strong covalent bonding, respectively [10].

Some of the widely researched amine-impregnated mesoporous materials are "molecular basket" sorbents (MBSs) which were prepared by immobilizing CO_2-philic polyethylenimine (PEI) on silica mesoporous molecular sieves (PEI-impregnated MCM-41, MCM-48, SBA-15, and KIT-6). Unlike other adsorbents, adsorption capacity of PEI-impregnated MCM-41 materials improved as temperature increased from 25 to 75 °C. However, these materials are not commercially available, and their preparation cost is very high; thus, their current use in CO_2 capture is not practical [11].

In addition to mesoporous materials, zeolites with microporous structures have also been used as supports for CO_2 adsorbents. Jadhav et al. studied monoethanol amine (MEA) modified zeolite 13X for CO_2 adsorption at different temperatures. In the study, first MEA modified 13X zeolite adsorbents had synthesized with MEA loadings of 0.5-25 wt.%. The adsorption capacities of adsorbents are measured in the temperature range 30-120 °C. The adsorbents show improvement in their CO_2 adsorption capacity and CO_2/ N_2 selectivity over those of the unmodified zeolite [12].

Other supports, for example, carbon-based supports, have also been studied. Plaza et al. impregnated PEI on supports produced from sewage sludge and air-oxidized olive stones (AOS). However any particular advantage or significant improvement of CO_2 adsorption capacity, measured at 25 °C, over non-PEI containing activated carbons, which were also tested in the same work, is not observed [13].

In order to overcome the thermal stability of amine-impregnated materials during desorption, aminosilanes were proposed to be covalently grafted onto the intrachannel surface of the mesoporous silicas through silylation. Several studies have been reported for synthesis of amine-grafted silicas for CO_2 capture using aminosilanes such as (3-aminopropyl)triethoxysilane (APS), *N*-[(3-trimethoxysilyl)propyl] ethylenediamine (2N-APS) and *N*-[(3-trimethoxysilyl)propyl] diethylenetriamine (3N-APS). The amine-grafted adsorbents exhibit comparatively higher adsorption rate and higher stability than the amine-impregnated ones [14].

Carbon materials, alumino-silicas such as zeolites, alumino-phosphates (AlPOs) and alumino-silico-phosphates (SAPOs), and, more recently, metal organic frameworks (MOFs) are considered as physical adsorbents for CO_2 capture [10].

Zeolites are highly ordered microporous crystalline materials. They are very promising for CO_2 adsorption. There are many advantages of zeolites such as low cost, relatively high stability and easy ion exchange. With the use of appropriate choice of Si/Al ratio, their gas–solid interaction energy can be tuned. So the potential for the selective gas separation can be increased while energy required for adsorbent regeneration is minimized [15]. Zeolites with low Si/Al ratio are taught to be the most promising zeolites for CO_2 adsorption [16-17].

The faujasite framework consists of sodalite cages, which are connected through hexagonal prisms with the pores arranged perpendicular to each other. Maurin et al. investigated the CO_2 adsorption capacity for several faujasite-type zeolites having different Si/Al ratios. Zeolites used for this study are dealuminated NaY (DAY, Si/Al = ∞), NaY (Si/Al = 2.4) and low silica NaX (NaLSX, Si/Al = 1). High purity (99.995%) carbon dioxide was used during the experiments. At low pressure, 13X (or NaX with Si/Al = 1.25) and NaY (Si/Al = 2.4) were claimed to be the most suitable adsorbents for both adsorption and desorption with favorable CO_2 adsorption isotherms. Dealuminated NaY showed at least 12 times lower adsorption capacity than NaY and NaLSX at 0.1 bar and room temperature [16].

Walton et al. demonstrated that substitution of Na cations by Rb, Cs, K and Li has a significant effect on the adsorption capacity in a wide range of CO_2 concentration. Bone dry CO_2 (minimum purity 99.8%) was used in the adsorption measurements. CO_2 capture capacity increased as Cs < Rb ≈ K < Li ≈ Na for Y zeolites. For X zeolites, the adsorption capacity for CO_2 increased in the order Cs < Rb < K < Na < Li (i.e. the order of decreasing ionic radii) [17].

Since high silica microporous materials contain less extra-framework cations than faujasite zeolites, they exhibit lower adsorption capacity [16-17].

When CO_2 stream is dry, zeolites generally operate without any loss in performance. Although low silica materials show high adsorption capacity and selectivity at low pressure,

they are very sensitive to the presence of water, which strongly inhibits the adsorption of CO_2. Thus, dehydration of flue gas prior to CO_2 capture is required [10].

Zukal et al., investigated the ability of hydrophobic high silica zeolites. Adsorption isotherms of carbon dioxide were measured at 273, 293, 313 and 333 K on cation-exchanged (Li+, Na+, K+, Cs+) MCM-22 zeolite with the molar ratio of Si/Al = 15 and a series of Na-MCM-22 of Si/Al molar ratios varying in the range from 15 to 40. For these forms of MCM-22 zeolite the heats of adsorption decrease with decreasing cation content. Moreover, similarly to X and Y zeolites, they show decreasing selectivity in the tests conducted with $CO_2 – N_2$ mixture as the temperature increases [18].

13X is the most widely investigated zeolite for the CO_2 adsorption. Chen et. al. prepared 13X for CO_2 adsorption, using bentonite as the raw material. The prepared zeolite showed a high BET surface area of 688 m^2/g with a high micropore volume (0.30 cm^3/g), and exhibited high CO_2 capture capacity (211 mg/g) and selectivity (CO_2/N_2= 37) at 25 °C and 1 bar. In addition, the material showed fast adsorption kinetics, and stable CO_2 adsorption–desorption recycling performance at both 25 and 200 °C [19].

T-type zeolite is an intergrowth-type zeolite of erionite (ERI) and offretite (OFF). Jiang et al. developed and observed the adsorption kinetics of T-type zeolites. Adsorption capacities of T-type zeolite nanoparticles are measured for pure CO_2, N_2 and CH_4 gases at 288, 298 and 313 K. The order of adsorption capacity is found to be $CO_2 > CH_4 > N_2$. Based on those preliminary results, selective adsorption tests were performed with binary CO_2-N_2 and CO_2-CH_4 mixtures over T-type zeolite nanoparticles. At 288 K and 100 kPa, the selectivity of CO_2/N_2 and CO_2/CH_4 of the T-type zeolite nanoparticles was 53.71 and 19.15 respectively. The dynamic adsorption experiments of binary gas mixtures showed that the synthesized T-type zeolite nanoparticles have promising adsorption capability and recyclability for the separation of CO_2 from CO_2/N_2 and CO_2/CH_4 gas mixtures, indicating their potential application to post-combustion CO_2 separation or natural gas purification process [20].

Another class of zeolites are alumino-phosphates (AlPO) and silica-alumino-phosphates (SAPO). AlPOs have a neutral overall framework. So they are expected to

behave as silicalite or dealuminated Y faujasite for CO_2 adsorption. Deroche et al. [21] used a combination of molecular simulation and microcalorimetry to show the CO_2 adsorption isotherm on AIPO-18. According to Deroche et al. AlPO-18 exhibits unfavorable adsorption isotherm. Similar to NaX and NaY, the framework of SAPOs is negatively charged and the overall charge is balanced by extraframework cations. In this case, it is expected to obtain a more favorable CO_2 adsorption isotherm with higher adsorption capacity at low CO_2 pressure, as reported by Castro et al. [22] for the proton form of SAPO-34. However, the CO_2 adsorption capacity on SAPO remains lower than that on X and Y faujasites [21- 22].

MOFs are porous crystalline materials composed of self-assembled metallic species and organic linkers. By changing the starting material, the material's properties can be changed. Using different organic ligands or metallic clusters would result in different pore sizes and shapes. This property of the metal organic frameworks makes them to be a good candidate particularly for storage of light gases (H_2, CH_4), and storage and separation of CO_2 [23].

Crucial contributions in the synthesis of novel MOFs and their CO_2 adsorption properties were made by Millward and Yaghi. They showed that at 35 bar, MOF-177-an extra-high porosity framework- can capture CO_2 about 2 times the amount of the benchmark materials such as zeolite 13X [24].

Caskey et al. reported a much higher and reversible adsorption capacity for pure CO_2 (23.6 wt.%, 5.36 mmol/g) at 0.1 bar and room temperature on Mg/DOBDC (or Mg-MOF-74) [25].

Most of the MOFs exhibit unfavorable adsorption isotherms at low pressures. They are fast CO_2 adsorbents but when a binary gas mixture CO_2/N_2 is used for adsorption most of the MOFs adsorbs more N_2 leading a low selectivity towards CO_2. MOFs are considered to be more suitable for CO_2 storage rather than the capture [10].

The CO_2 adsorption capacity and the CO_2/N_2 selectivity for most MOFs are very low and decreases significantly with the increasing temperature. Barcia et al. had studied single and multicomponent fixed-bed adsorption of CO_2, N_2, and CH_4 on crystals of MOF-508b.

Adsorption equilibrium was measured at temperatures ranging from 303 to 343K and partial pressures up to 4.5 bar. At single component tests it is seen that CO_2 is adsorbed much more than CH_4 and N_2, but CO_2 adsorption decreases significantly when the temperature is increased. This situation is same with binary test; although CO_2 is adsorbed more, with increasing temperature the CO_2/N_2 and the CO_2/CH_4 selectivity decreases drastically [26].

Li and Yang, when working on H_2 storage capacity of MOFs, showed that being exposed to water vapor unstabilizes the MOF structure. H_2O vapor adsorption studies done by Li and Yang showed that MOF-177 adsorbed up to 10 wt.% H_2O, and 65% of that cannot desorb from the MOF at room temperature [27].

The unstability of the MOF structure raised concerns which lead the discovery of a new class of MOFs. These zeolite-like MOFs (ZMOFs) called as zeolitic imidazolate frameworks (ZIF). ZMOFs are crystalline porous materials which are developed to combine the highly desirable properties of zeolites and MOFs, such as microporosity, high surface areas, and exceptional thermal and chemical stability. The work done by Park et al. demonstrated the permanent porosity (Langmuir surface area 1.810 m^2/g), high thermal stability (up to 550 °C), and remarkable chemical resistance to boiling alkaline water and organic solvents of ZIF-8 and ZIF-11, which are synthesized as crystals by copolymerization of Zn(II) [28].

A series of ZIFs (ZIF-68, -69, -70, -78, -79, -81, -82, -95, and -100) have been examined for their potential to separate CO_2 from CH_4, CO, O_2, and N_2. Crucial improvement was observed in terms of CO_2/N_2 selectivity, which increased up to 50 for ZIF-78. However, at low CO_2 partial pressure the CO_2 adsorption capacity was still low [29].

COFs are crystalline organic porous materials without metal ions. They are developed to overcome the hydrophilic behavior of zeolites, MOFs and ZMOFs. Furukawa et al. reported high CO_2 adsorption capacities (1190 mg/g) for a series of COFs for high partial pressure of CO_2, but adsorption at low partial pressure of CO_2 appeared to be significantly lower than for Mg-MOF-74 [30].

Carbon based materials are widely investigated as CO_2 adsorbents because of their availability, low cost and high thermal stability. Carbons as CO_2 adsorbents have been studied for a long time and have found commercial applications [10].

Carbon molecular sieves (CMS) are carbonaceous materials with a narrow pore size distribution. They have a selective adsorption capacity of certain components of a mixture. They can discriminate molecules based on their size, shape or difference in adsorption equilibrium or, even, adsorption rate. CMS are commonly prepared from a variety of carbonaceous materials such as cellulosic precursors, coals, carbon fibers, resins, etc. [31].

Wahby et al. studied the CO_2 adsorption ability of a series of commercial carbon molecular sieves (CMS), prepared from different polymeric precursors. The CMSs used for this study cover a wide range of porosity, from purely microporous carbons to samples containing wide micropores with a certain proportion of mesoporosity. Studies are conducted at atmospheric pressure (1 bar) and at three different temperatures (273, 298 and 323 K).The presence of a well-developed microporosity and large volume of narrow micropores have shown a high CO_2 adsorption capacity. On the other hand, narrow micropores seem to be the key factor leading to a maximum capacity of CO_2 adsorption, even at temperatures close to that of anthropogenic emissions of CO_2 [31].

CNTs (Carbon Nanotubes) are relatively new adsorbents which occupies an interesting positions in carbon-based adsorptive materials due to their highly porous and hollow structure, large specific surface area, light mass density and strong interaction between CNTs and pollutant molecules. In order to explore the adsorption behavior of an equimolar CO_2/CH_4 mixture in CNTs, Grand canonical Monte Carlo (GCMC) simulations were performed by Huang et al. Five CNTs with diameters varying from 0.678 to 1.356 nm were chosen for the simulations. Simulations are done at seven different temperatures (283-343 K), and pressures (1-30 MPa). The simulations demonstrated that the CNTs have a preferential CO_2 adsorption ability from the binary mixture. With increasing diameter, CO_2 adsorption in the CNTs also increases. However for different pore sizes, the absolute amount of adsorbed CH_4 does not change. The adsorption behavior of CNTs with diameters less than 1.1 nm had not much affected by the temperature and pressure changes, whereas in larger CNTs the adsorption behavior changes with temperature and pressure significantly.

The CNTs demonstrated in this study showed a higher selectivity of CO_2 than other materials (activated carbons, zeolites 13X, and metal-organic frameworks) reported in the literature. For example, in case of (6, 6) CNT at 343 K and 1 MPa, the selectivity reaches 11.2, larger than that reported for activated carbon [32].

2.2. Activated Carbon

Activated carbon is among the most useful adsorbents used in industries. Because of its well-developed pore structure, high surface area and good mechanical characteristics, activated carbon can be used in many adsorption processes ranging from liquid to gas. Activated carbons may originate from the wide selection of materials like santhracite, bituminous coal, petroleum pitch fiber, and coal tar pitch, and are activated with different activation procedures, such as CO_2 activation, steam (physical) activation, and via using various oxygenation, nitrogenation, hydrogenation, etc. agents, i.e. chemical activation. Because of the different origins and preparation methods, different ACs have significantly different physico-chemical properties, including pore structure, surface properties and ash content. Which parameters influence CO_2 adsorption capacity of AC-based materials and how they influence the adsorption kinetics are still in research [33].

2.2.1. CO_2 Adsorption on Activated Carbon

CO_2 adsorption capacity of activated carbon are highly affected by the surface chemistry and pore structure [33-34]. The pore size distributions of activated carbons vary from micropore to macropore and easily controlled by changing the preparation and activation conditions [33].

Shahkarami et al. studied the effect of activation method on CO_2 adsorption. Three activated carbons used in this study were prepared from biochar, obtained from fast pyrolysis of white wood, using three different activation methods of steam activation, CO_2 activation and KOH activation. Their CO_2 adsorption behavior was studied in a fixed-bed reactor set-up at atmospheric pressure, temperature range of 25–65 °C and inlet CO_2 concentration range of 10–30 mol% in He to determine the effects of the surface area, porosity and surface chemistry on adsorption capacity of the samples. Characterization of the micropore and

mesopore texture was carried out using N_2 and CO_2 adsorption at 77 and 273 K, respectively. The steam and CO_2 activated carbons showed the similar pore structures and had high mesopore volumes whereas KOH activated carbon had the highest ultra-micropores and super-micropores volume while its mesopore volume was negligible. The steam, CO_2 and KOH activated carbons had the BET surface area of 840, 820 and 1400 m^2/g, respectively and their total pore volumes are estimated to be 0.55, 0.45 and 0. 62 cm^3/g, respectively. The KOH activated carbon had the highest CO_2 adsorption capacity of 1.8 mol/kg due to its microporous structure and high surface area under the optimized experimental conditions of 30 mol% CO_2 and 25 °C. The performance of the adsorbents in multi-cyclic adsorption process was also tested and the adsorption capacity of KOH and CO_2 activated carbons remained remarkably stable after 50 cycles with low temperature (160 °C) regeneration [35].

Lee and Park investigated a commercially available activated carbon fiber for its CO_2 adsorption capacity and modified it further with chemical activation to obtain higher CO_2 adsorption capacity. Chemical activation (with KOH at a fixed activation temperature of 900 °C for 1 h and various KOH/ACF weight ratios ranging from 1 to 4) of ACF increased the total pore volume and specific surface area to 1.124 cm^3/g (KOH/ACF weight ratio of 2) and 2318 m^2/g (KOH/ACF weight ratio of 4), respectively. Compared to ACF, the total pore volume and specific surface area were improved by factors of 2.5 and 2.3, respectively. The highest CO_2 adsorption capacity observed on the AFC modified with a KOH/ACF ratio of 3. In this study, it is seen that the CO_2 adsorption capacity was strongly affected not by the specific surface area or micropore volume but by the ultra-micropore size distribution [36].

Yin et al. also proved that ultra-micropores are more effective in CO_2 adsorption compared to other surface properties. Three bio-ACs (termed coconut-AC, apricot-AC and date-AC according to their origin) and one coal-AC were studied under conditions of pressure swing adsorption (PSA, 273–293 K and CO_2 pressures of 0.01–0.10 MPa). They were ground and sieved to 20-40 mesh, and then acid-washed with 10% HCl and 12% HF at 60 °C for 24 h. The treated ACs were washed with de-ionized water until pH reached 7 and dried at 150 °C for 2 h. Results indicate that the surface properties of AC, i.e. the type and abundance of the oxygen-containing functional groups, have little effect on CO_2 adsorption, while the ultra-micropore (<0.7 nm) volume has a significant effect on CO_2 adsorption capacity. The ash in biomass-derived AC, mainly K compound, has a positive

effect on CO_2 adsorption while the ash in coal-derived AC, mainly Ca, Si, Al and Fe compounds, are inert to CO_2 adsorption [33].

Like pore structure of activated carbons, the functional groups on the activated carbon surface can also be easily controlled using different treatments. The incorporation of various basic groups on activated carbon has been actively investigated for enhancing the CO_2 affinity by increasing the CO_2 adsorption capacity [34]. It is expected that the introduction of Lewis bases onto the activated carbon surfaces may increase the capture performance due to acidic role of CO_2, which is a weak Lewis acid. [37].

The acidic character of activated carbon surfaces come from the oxygen containing surface groups. These groups which are mainly present on the outer surface or edge of the basal plane contribute toward the chemical nature of the carbon. Basicity of activated carbon can be associated with resonating π-electrons of carbon aromatic rings that attract protons, and basic surface functionalities (e.g., nitrogen containing groups) that are capable of binding with protons. Large number of oxygen containing acidic groups on carbon surface overshadows the contribution of resonating π-electrons to carbon basicity. One of the ways used to increase the basicity of activated carbon is to remove/neutralize the acidic functionalities, and the other way is to replace acidic groups with proper basic groups, such as basic nitrogen functionalities [37].

High temperature (>700 °C) heat treatment under atmosphere might be used to selectively remove most of surface acidic functionalities from the activated carbon surface. Heat treatment of carbon under hydrogen can increase carbon hydrophobicity by removing hydrophilic surface functionalities [37].

Ammonia treatment is considered to be an effective way to add nitrogen functionalities to activated carbon surface to make it more alkaline. Shafeeyan et al., used a commercial palm shell-based granular activated carbon (GAC) as starting material for the preparation of CO_2 adsorbent and investigated the effect of two different ammonia treatment: direct ammonia treatment for which samples are only heat treated under nitrogen and amination of oxidized samples for which preliminary air oxidation is applied prior to the introduction of ammonia. Ammonia modifications were done in a tubular quartz reactor under gaseous

ammonia flow. It was found that in both modification techniques, the presence of nitrogen functionalities on carbon surface generally increased the CO_2 adsorption capacity. The results indicated that oxidation followed by high temperature ammonia treatment (800 °C) considerably enhanced the CO_2 uptake at higher temperatures [38].

Eucalyptus wood was chosen to produce activated carbon by chemical activation with H_3PO_4 as an adsorbent for CO_2 adsorption. It was subjected to thermal treatment with the ammonia solution at 400 and 800 °C in order to improve CO_2 capture. The textural and surface characteristics of the prepared activated carbons were determined from the analysis of N_2 adsorption isotherms, elemental analysis, Fourier Transform Infrared spectroscopy (FT-IR) and scanning electron microscopy (SEM), Boehm titration and X-ray photoelectron spectroscopy (XPS). AC modified at 800 °C had the highest BET surface area, micropore volume and total pore volume while AC modified at 400 °C had the lowest. The adsorption behavior of CO_2 onto carbon samples was experimentally evaluated by volumetric method at temperatures ranging from 288 to 348 K and pressure range of 0-16 bar. The CO_2 adsorption capacity achieved by modified carbon was 3.22 mmol/g at 1 bar and 303 K which became more than the virgin carbon (2.9 mmol/g).

As it is mentioned, there are several methods by which activated carbons can be modified to improve their adsorption capacity, including oxidation, heat treatment, chemical treatment with acidic, basic solutions or metallic species, etc. Most prominent method to enhance the CO_2 adsorption capacity is by promoting basic species on the surface of activated carbon through chemical impregnation. Lee et al. studied the effect of hindered ammine impregnation on palm shell-based activated carbon (AC) with BET surface area of 882 m^2/g, which is a product of Bravo Green Sdn. Bhd. In their work, equimolar amounts of three types of sterically hindered amines (e.g. 2-amino-2-methyl-1, 3-propanediol, 2-amino-2-methyl-1-propanol and 2-(methylamino)ethanol) were used. Impregnation is done by soaking a given amount of activated carbon in an amine solution. Impregnated activated carbon had higher adsorption capacity than virgin activated carbon despite the dramatic decrease in surface area during impregnation. Among the three investigated amines, 2-amino-2-methyl-1-propanol showed the highest CO_2 adsorption capacity [40].

The enhancement of CO_2 adsorption on ACs with high surface area modified by using microwave irradiation under N_2 or H_2 flows (denoted as NAC and HAC, respectively) and ammonia impregnation (denoted as AAC) is investigated by Zhang et al. The modified ACs were characterized, and their surface chemical properties determined separately by FTIR, Boehm titration and X-ray photoelectron spectroscopy (XPS) methods. The amounts of the surface basic groups on the ACs followed the order: NAC>HAC> AAC > AC, suggesting that the use of microwave irradiation in the atmosphere of N_2 to modify the carbon surfaces can make the surface basic group concentration of the ACs the highest among those tested. As a consequence, the modified ACs had higher adsorption capacities of CO_2 compared to the original AC. And the more the total basic groups on the surfaces of the carbon, the higher its adsorption capacity of CO_2. The amounts adsorbed of CO_2 on these ACs followed the same order: NAC>HAC> AAC > AC. The amount adsorbed on the NAC was up to 3.75 mmol/g at 1 atm and 298 K, having an increase of 28% in comparison with the original AC [41].

The effect of impregnation of activated carbon with Cr_2O and Fe_2O_3 and promotion by Zn^{2+} on its carbon dioxide adsorptive properties was studied by a volumetric adsorption apparatus at ambient temperature and at low pressures by Somy et al. Norit RB3 was used as the raw AC material. Two types of impregnation method were applied for zinc promotion, slurry and solution impregnation. In conventional solution method, zinc deposition on activated carbon surface is done by using an aqueous solution of zinc nitrate. In slurry impregnation method, aqueous slurry of zinc hydroxide carbonate is used. In order to observe the effect of washing with distilled water after impregnation, some of the samples were prepared without washing stage. Their experimental results indicated Cr_2O is an effective metal oxide species which can increase CO_2 adsorbed amount on the impregnated activated carbon. The obtained adsorption isotherms showed that Cr_2O impregnation increased the amount of CO_2 adsorbed on the samples by 20% compared to raw activated carbon. Fe_2O_3 was not found to be an effective agent for activated carbon modification. Moreover, it is reported that slurry impregnation method led to a higher CO_2 adsorption capacity compared to solution impregnation method. Samples prepared by co-impregnation of two metal species showed more adsorption capacity than samples impregnated by just one metal species. Washing the impregnated samples with water resulted in 15% increase in CO_2 adsorption capacity [42].

Caglayan and Aksoylu had studied CO_2 adsorption on chemically modified activated carbon. HNO_3 oxidation, air oxidation, alkali impregnation and heat treatment under helium gas atmosphere were the methods used to improve the CO_2 adsorption capacity of a commercial activated carbon (Norit ROX 0.8). Their results indicated the enhancement in carbon dioxide adsorption capacities of air oxidized and nitric acid oxidized AC samples impregnated with Na_2CO_3. The mass uptakes of the adsorbents at 20 bars and 25 °C are increased by 8 and 7 folds, respectively. The mass uptakes of the adsorbents at 1 bar were increased 15 and 16 folds [8].

Guo et al. studied on a novel PEI-K_2CO_3/AC sorbent obtained with the impregnation of 25 wt.% K_2CO_3 and 25 wt.% PEI on activated carbon. The CO_2 capture performance and the multi-cycle operation behavior of PEI-K_2CO_3/AC were compared with those of K_2CO_3/AC with K_2CO_3 loading of 58 wt.% and PEI/AC with PEI loading of 43 wt.%. The PEI-K_2CO_3/AC was found to show a high CO_2 capture capacity of 3.60 mmol CO_2/g at 60 °C. The PEI-K_2CO_3/AC was proved to be regenerable and stable with a retained CO_2 capture capacity of 3.42 mmol CO_2/g after 5 cycle adsorption–desorption tests. PEI-K_2CO_3/AC showed superiority on CO_2 capture capacity and long-term stability over K_2CO_3/AC and PEI/AC [43].

CO_2 adsorption on activated carbon seems to be well-favored at high pressures and low temperatures. These limitations may not be suitable for low pressure CO_2 capture from flue gas treatment. So, nowadays the strategy for CO_2 adsorption on carbonaceous materials is to increase the strength of CO_2 interactions at low partial pressures via surface modification.

2.2.2. CH_4 Adsorption on Activated Carbon

Natural gas is one of the alternatives to petroleum based fuels. However, it is necessary to find the safe and economical method to facilitate the large scales of NG. Adsorbed natural gas (ANG) technology is based on the adsorption of natural gas in porous materials. The studies on the use of ANG have focused on the development of new materials, particularly carbon-based adsorbents which could improve adsorption capacity [44].

Yang et al. studied three kinds of activated carbon prepared by coconut-shells. The differences of these three activated carbons results from their carbonization stages. While first one is purged by nitrogen for 30 min before carbonization (denoted W-AC), the other two put into phosphoric acid solution (denoted P-AC), and KOH solution (denoted K-AC) before carbonization. P-AC had the highest micropore surface area (1922 m^2/g) and highest micropore volume (0.68 cm^3/g) while K-AC had the lowest. The adsorption capacities of CH_4, CO_2, N_2 and O_2 over the activated carbons are tested at 25 °C in the pressure range of 0−220 kPa. The CO_2 adsorption capacities of all samples increased with the increasing pressure at 25 °C. However, the behavior of CH_4 adsorption was not same as that of CO_2 adsorption, especially over the P-AC sample. The amount of CH_4 adsorbed over the P-AC sample was very small, implying that P-AC was not an appropriate adsorbent for CH_4. The results revealed that all the activated carbons had high CO_2 adsorption capacity, one of which had the highest CO_2 adsorption value of 2.55 mmol/g (P-AC) at 200 kPa while the highest adsorption capacity for CH_4 of the activated carbons can only reach 1.93 mmol/g (K-AC) at the same pressure. The N_2 and O_2 adsorption capacities of all samples were almost the same and increased slowly with the change of pressure [45].

2.2.3. Selective Adsorption on Activated Carbon

CO_2 removal from a gas mixture is required for different industrial purposes. For example, removal of CO_2 contamination from natural gas sources to satisfy pipeline specifications or to produce Liquefied Natural Gas (LNG) [46], removal of CO_2 for purification of the bio-hydrogen and biogas [47], and for separation of CO_2 from the other gases present in the flue gas of a power plant [48]. So that, the selective adsorption studies in the literature mainly focuses on CO_2 separation from flue gas mixture, and determination of CO_2/CH_4 and CO_2/N_2 selectivity values of the adsorbents.

In a study made by Grande et al. activated carbon was used as selective adsorbent for separation of CO_2 from CO_2/CH_4 mixtures at high pressures. The activated carbon used for the research is mainly microporous with only very small fraction of macro-mesopores indicated by the t-plot values of 2180 m^2/g and 1.07 cm^3/g for the micropore-area and -volume, respectively, and only 27 m^2/g for the external area which include the areas of the pores. The experimental setup contains three mass flow controllers, a stainless steel column

with two temperature sensors, a pressure regulator and a continuous detection unit at the outlet. Detection unit consists of a gas analyzer with an Infra-Red detector. Binary adsorption measurements of 10 and 20% CO_2 balanced with CH_4 were carried out at three different pressures: 500, 2500 and 5000 kPa. It is found that although the amount adsorbed of CO_2 is higher than the amount adsorbed of CH_4, the amount of adsorbed CH_4 is still too high to use this adsorbent for selective adsorption [46].

Gil and co-workers studied the performance of three activated carbons (No1KCla-600, No1KClb-1000 and No2OS-1000), synthesized from phenol–formaldehyde resins, as potential adsorbents for CO_2 capture from bio-hydrogen and biogas streams. Adsorption–desorption cycles by means of temperature swings were conducted at ambient temperature and atmospheric pressure with CO_2/H_2 (40/60 and 70/30 vol.%) and CO_2/CH_4 (50/50 vol.%) binary gas mixtures in a purpose-built fixed-bed set-up. Their adsorbents presented high CO_2/H_2 and CO_2/CH_4 selectivity values, were easily completely regenerated and did not lose capacity after multiple cycling. The highest CO_2/CH_4 selectivity value (4.26) was observed for the No2OS-1000 adsorbent while the No1KCla-600 adsorbent gave the greatest values of CO_2 capture capacity reaching 2.11 and 2.03 mmol/g for 70/30 CO_2/H_2 and 50/50 CO_2/CH_4, respectively [47].

A microwave-activated carbon (MAC) with surface area of 671.17 m^2/g and total pore volume of 0.333 cm^3/g was used in the study by Yi et al. Pure gas isotherms for CO_2, CH_4 and N_2 measured by using a conventional volumetric apparatus, with a pressure transducer equipped with a vacuum system, while the adsorption temperature was maintained with a stirred thermostatic water bath. The Toth equation and the Langmuir model were used to correlate the experimental data. The highest adsorption capacity was observed for CO_2 while the lowest adsorption capacity was measured for N_2. In order to investigate selective adsorption, the adsorption amount of multi component systems was predicted at different equilibrium pressures and compositions by the extended Langmuir and the extended classical Toth models. The selectivity for the binary mixtures: CO_2/CH_4, CO_2/N_2 and CH_4/N_2 were estimated by using a methodology based on the determination of the equation of state for the Gibbs free energy of desorption of the solid adsorbent. The highest separation factors were obtained for the CO_2/N_2 and CO_2/CH_4 systems. It can be predicted that MAC has potential to be used in the separation of CO_2/N_2 and CO_2/CH_4 mixtures [49].

Hao et al. worked on physically activated and chemically activated carbons. The HTC biomass was used as the precursor. HTC biomass was activated to Physically Activated Carbon (PAC) under a steady flow of CO_2. CAC (Chemically activated carbon) was prepared by treating carbonized beer waste hydrothermally with H_3PO_4 followed by a heat treatment under N_2 flow. Both PAC and CAC showed high CO_2 adsorption capacity. The adsorption of CO_2 at 10 kPa and 0 °C was the highest for the PAC (1.45 mmol/g). CAC prepared had only half of the ultramicropore volume of the PAC, however, it displayed higher CO_2/N_2 selectivity [50].

Lopes et al. provided adsorption equilibrium and kinetics of the pure gases in a steam methane reforming (SMR) off-gas, H_2O, CO_2, CH_4, CO, N_2, and H_2, on two different adsorbents, activated carbon and zeolite. Data were collected at 303–343 K and 0–7 bar. Water adsorption was only measured on the activated carbon at 303 K. The adsorption capacity sequence of the activated carbon was found to be: $H_2O>CO_2>CH_4>CO>N_2>H_2$, while for the zeolite it is $CO_2 >CO>CH_4>N_2>H_2$. The amount of adsorbed carbon dioxide at high pressures was essentially the same for ACs and zeolite. At low CO_2 partial pressure, activated carbons exhibit lower adsorption capacity and selectivity than zeolites due to their less favorable adsorption isotherms. Although carbon based materials have a hydrophobic character, CO_2 adsorption ability of ACs is adversely affected by the presence of water vapor. H_2O adsorption makes the regeneration of the activated carbon easier [51].

Guo and co-workers analyzed the CO_2 adsorption characteristics of K_2CO_3/AC for pure CO_2, binary mixture of N_2-CO_2 (99:1), and ternary mixture of N_2-CO_2-H_2O (97:1:2) at temperatures in the range of 293–333 K. The adsorption capacity of K_2CO_3/AC decreased with the increasing temperature. They also observed that K_2CO_3 loading on AC affected the surface properties in two opposite ways: it decreased the activation energy owing to improvement of the basicity of the support, but it also decreased the number of adsorption sites due to the reduction in surface area and pore volume. The best K_2CO_3 loading amount for optimal CO_2 capture performance was verified and 30 wt.% K_2CO_3 loaded AC's CO_2 capture behavior was studied. In pure CO_2 atmosphere, the adsorption capacity was found to be 64.75 mg CO_2/g adsorbent. The binary mixture of N_2-CO_2 (99:1) and ternary mixture of N_2-CO_2-H_2O (97:1:2) exhibited capture capacities of 38.58 mg/g and 64.74 mg/g, respectively [52]. More detailed understanding of CO_2 sorption by K_2CO_3/AC deserves

further investigation, regarding the physical adsorption process on AC and effect of K_2CO_3 and water vapor on its CO_2 adsorption behaviors.

2.3. Adsorption Isotherms Models

Adsorption isotherms are functions which link the amount of adsorbate on the adsorbent, with its pressure (if gas) or concentration (if liquid), at a constant temperature and pH. Adsorption equilibrium defined as the ratio between the adsorbed amount with the remaining in the solution is established when an adsorbate has been contacted with the adsorbent for sufficient time, and its adsorbate concentration in the bulk solution is in a dynamic balance with the interface concentration [53].

2.3.1. Langmuir Isotherm Equation

The Langmuir adsorption isotherm equation was initially developed to describe the adsorption of gases onto clean solids. This equation can be derived theoretically based on evaporation and condensation rates. Langmuir equation assumes a uniform surface, constant temperature, and monolayer adsorption [54]. The equation is:

$$Q_A = \frac{K_{eq}^A P_A}{1 + K_{eq}^A P_A} \tag{2.1}$$

where Q_A is the fractional occupancy of the adsorption site, K_{eq}^A is equilibrium constant and P_A is partial pressure of the adsorbate [54].

2.3.2. Freundlich Adsorption Equation

The Freundlich adsorption isotherm equation is the oldest of the non-linear adsorption isotherms involving heterogeneous surfaces [54]. It is mathematically expressed as

$$\frac{x}{m} = KP^{1/n} \tag{2.2}$$

where x is mass of adsorbate, m is mass of adsorbent, P is equilibrium pressure of adsorbate, K and n are constants for a given adsorbate and adsorbent at a particular temperature [54].

At high pressure 1/n = 0, hence extent of adsorption becomes independent of pressure [54].

2.3.3. Temkin Adsorption Equation

Temkin Isotherm is derived from the Langmuir Isotherm by inserting the condition that heat of adsorption decreases linearly with surface coverage [54]. Mathematical equation is:

$$Q=c_1 \ln(c_2 P) \tag{2.3}$$

where Q is the fractional occupancy of the adsorption site, P is equilibrium pressure of adsorbate, and c_1 and c_2 are constants [54].

2.3.4. Toth Adsorption Equation

Toth Equation describes systems with submonolayer coverage and is valid at the low and high ends of the pressure range [54]. Toth equation can be represented by

$$N= \frac{mP}{(b+P^t)^{1/t}} \tag{2.4}$$

where N is the amount adsorbed, m is the saturated amount adsorbed, P is the equilibrium pressure, b is the equilibrium constant, and t is the parameter that indicates the heterogeneity of the adsorbent [54].

2.3.5. The Dubinin-Astakhov Equation

Competitive or multilayer adsorption on microporous adsorbents can be described by Dubininin-Astakhov Equation [54]. It can be written as:

$$W=W_0 \exp\left[-\left(\frac{A}{E}\right)^n\right] \tag{2.5}$$

where W is the volume adsorbed, W_0 is the limiting micropore volume, E is the characteristic energy of the system, n is the heterogeneity parameter, and A is the adsorption potential. The adsorption potential A is given by

$$A=RT \ln\left(\frac{P_s}{P}\right) \tag{2.6}$$

where R is the universal gas constant, T is the equilibrium temperature, and P_s is the saturation pressure. Dubinin-Astakhov model applies to the adsorption equilibrium of several vapors and gasses including CO_2 on micro porous activated carbons [54].

2.3.6. The Dubinin-Radushkevich Equation

For a large variety of microporous carbons such as activated carbons, the adsorption data can be fitted to Equation (2.5) with n=2, which corresponds to Dubinin-Radushkevich equation which can be written as:

$$W=W_0 \exp\left[-\left(\frac{A}{E}\right)^2\right] \tag{2.7}$$

2.4. Pseudo-first Order and Pseudo-second Order Kinetic Models

A predictive model using thermodynamic equilibrium and reliable kinetic parameters may provide a method for estimating the adsorption dynamics and CO_2 adsorption column sizing without extensive experimentation. It is possible to fit the kinetic data to both pseudo-first and pseudo-second order models aiming to determine the correlation appropriate

reaction order for the adsorption processes based on goodness-of-fit, i.e. R^2-coefficient values [55]. The linear form of the pseudo-first order kinetic model is given by;

$$\ln(q_e - q_t) = \ln(q_e) - k_1 t \tag{2.8}$$

where q_e and q_t are the amount adsorbed in mg/g at equilibrium time and any time t where q_e and q_t are the amount adsorbed in mg/g at equilibrium time and any time t (min), respectively, and k_1 is the pseudo-first order rate constant (min^{-1}). The rate constant can be obtained from the slope of ln ($q_e - q_t$) versus t plot [55].

The linear form of the pseudo-second order kinetic model can be expressed as;

$$\frac{t}{q_t} = \frac{1}{k_2 q_e^2} + \frac{t}{q_e} \tag{2.9}$$

where k_2 is the pseudo-second order rate constant ($mgg^{-1}min^{-1}$) and the plot of t/q_t versus t gives the values of k_2 and q_e [55].

3. EXPERIMENTAL WORK

3.1. Materials

3.1.1. Chemicals

The chemicals used for adsorbent preparation are listed in Table 3.1.

Table 3.1. Chemicals used in adsorbent preparation.

Chemicals	Formula	Source	Molecular Weight (g/mole)
Activated Carbon (ROX 0.8)	C	NORIT	12.00
Hydrochloric Acid	HCl	Merck	36.40
Nitric Acid	HNO_3	Merck	63.00
Potassium Carbonate	K_2CO_3	Merck	138.21

3.1.2. Gases

All the gases were produced by Birleşik Oksijen Sanayi (BOS) and Linde Gas. The specifications and applications of the gasses used in this study are summarized in Table 3.2.

Table 3.2. Specifications and applications of the gases used.

Gas/Standard	Specification	Application
Carbon dioxide	99.995%	Pure/Selective CO_2 Adsorption, DSMS Calibration
Helium	99.999%	DSMS Calibration
Methane	99.5%	Pure/Selective CH_4 Adsorption, DSMS Calibration
Nitrogen	99.99%	Adsorbent Preparation
Oxygen	99.99%	Adsorbent Preparation

3.2. Experimental Systems

The experimental systems can be divided into three groups:

- Adsorbent Preparation Systems: The set-ups used for adsorbent modification and incipient-to-wetness impregnation.

- Adsorbent Characterization Systems: The analytical and spectroscopic techniques and the systems used to characterize the physical and microstructural properties of the adsorbent samples prepared.

- Adsorption System: The continuous adsorption system which includes gas and liquid flow control, temperature controlled transfer lines, and HIDEN ISOCHEMA IGA-003 Intelligent Gravimetric Analyzer-HIDEN HPR-20 QIC EGA Mass

Spectrometer system produced by Hiden Isochema Warrington, England (IGA-DSMS).

3.2.1. Adsorbent Preparation Systems

The system used for HCl and HNO_3 treatments of activated carbon consists of an Electro-mag heating mantle, a soxhlet apparatus, a condenser, and a round bottom flask and a beaker. The air treatment system employs a vertical Lenton furnace having a Eurotherm temperature controller. The nitrogen and oxygen gases used for air treatment were fed to the system through gas regulators, and the flow rate of both gasses were controlled by mass flow controllers.

A system consisting of Retsch UR1 ultrasonic mixer, a vacuum pump, a Büchner flask and a MasterFlex computerized-drive peristaltic pump was used for adsorbent modification through impregnation. Air and HNO_3 treated samples used in the current study were further modified by impregnation of K_2CO_3 solution via incipient-to-wetness impregnation technique (Figure 3.1).

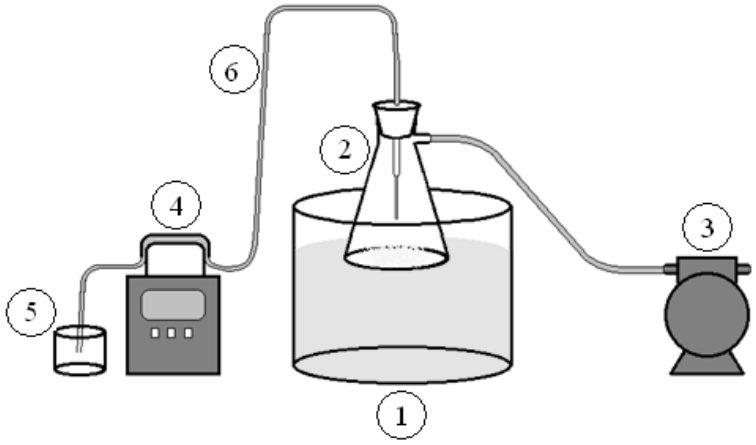

Figure 3.1. Schematic diagram of the impregnation system (1. Ultrasonic mixer, 2. Büchner flask, 3. Vacuum pump, 4. Peristaltic pump, 5. Reactant storage tank, 6. Silicone tubing).

3.2.2. Adsorbent Characterization Systems

Scanning Electron Microscopy (SEM). Micrographs of the adsorbent samples were taken by SEM and SEM-EDX (Energy Dispersive X-Ray) to analyze their microstructural properties and metal dispersion. The tests were conducted in a Philips XL 30 ESEM-FEG system, having a maximum resolution of 2 nm. Secondary electron (SE) and back-scattered electron images were obtained for modified activated carbon adsorbents. The analyses were performed at the Advanced Technologies Research and Development Center of Boğaziçi University.

3.2.3. Adsorption System

CO_2 and CH_4 adsorption and selective adsorption tests of the adsorbents were conducted by using IGA-DSMS system (Figure 3.2). The adsorption/desorption isotherms were obtained within 0-1000 mbar and 0-5000 mbar pressure ranges at three different temperature values; room temperature (RT), 120 °C and 200 °C. The concentration of the gases leaving the adsorption unit was analyzed by DSMS.

IGA is designed and programmed to work in two modes; those are dynamic and static modes. In static mode, the gases that were supplied by pressurized tubes were passed through the gas flow regulators and sent directly to IGA. Since there are no mass flow controllers between the IGA inlet and gas flow regulators, there is no way to control or manipulate the flow rate and the feed composition in the static mode; only the pressure level of the supplied gas fully controlled by IGA. Therefore, the static mode cannot be used for selective adsorption studies. In this study, dynamic mode of the IGA was used since dynamic mode allows flow rate measurements to be made with gas mixtures, which are essential in many practical applications.

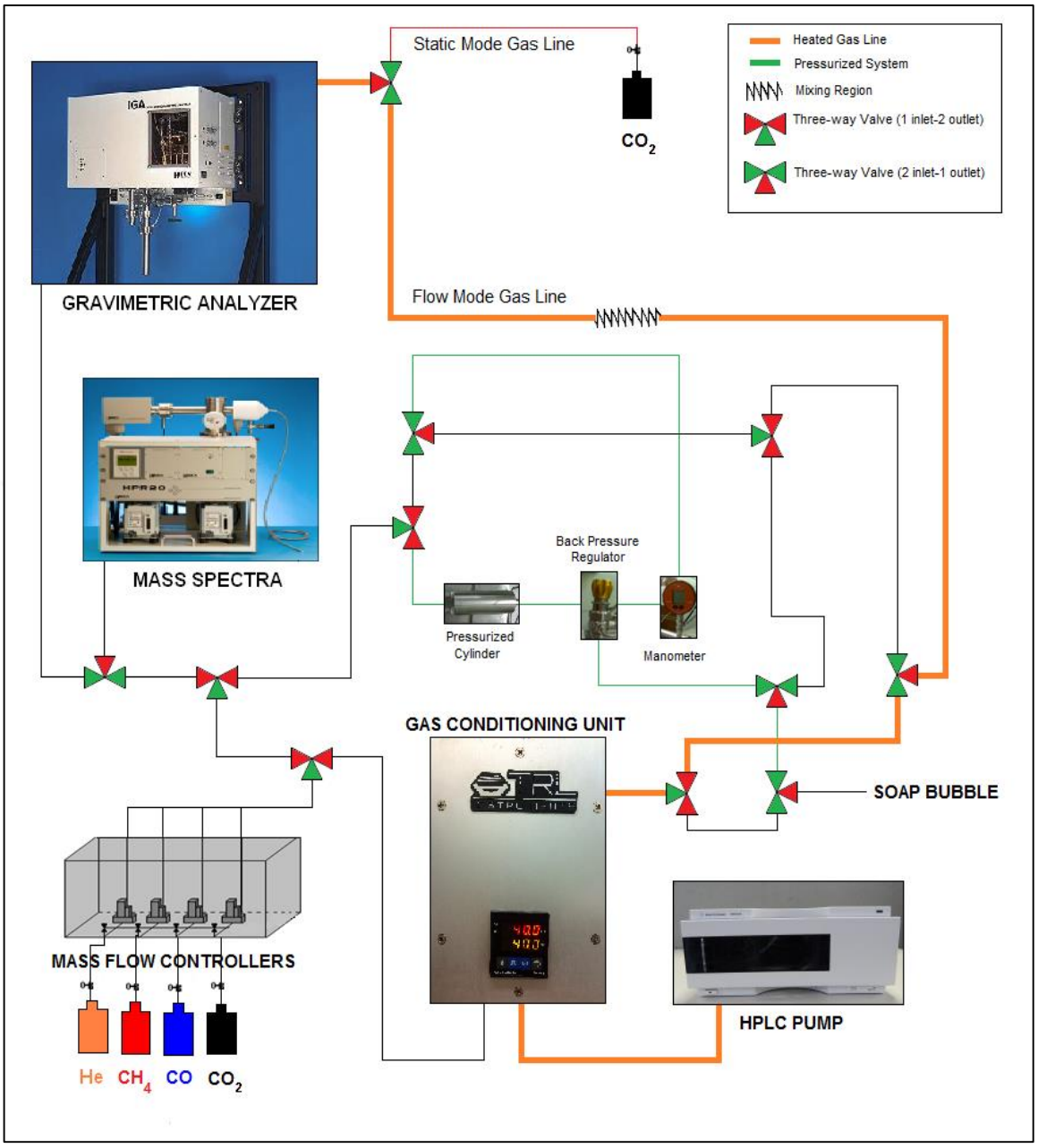

Figure 3.2. Experimental setup for adsorption experiments.

The feed section of the IGA-DSMS system has mass flow control systems, 1/4", 1/8" and 1/16" stainless steel tubing, valves and fittings for controlling both the composition of the gas mixtures, and the flow rates of all the gaseous species (i.e. carbon dioxide, methane, and helium) as well as the gas mixtures fed to the system,. The gases that were supplied by pressurized cylinders were passed through the gas flow regulators which are set to 2000 mbar for 0-1000 mbar range adsorption/desorption tests and set to 7000 mbar for 0-5000 mbar range adsorption/desorption tests, and the flow rates of the gases were regulated by

calibrated Brooks Instrument mass flow controllers. To avoid possible back-pressure fluctuations, on-off valves were placed in front of the mass flow controllers. It was possible to meter the flow of individual species and adjust desired feed ratios since each gas was fed from its independent line. The gases were then introduced to a primary mixing zone in order to obtain the homogeneous and stable flow of gas mixture. The gas mixture were sent to a three way valve with one inlet and two outlets which provides an opportunity for conducting adsorption tests in the presence of moisture. Water addition to the gas mixture was accomplished with HPLC pump and mixing and heating were accomplished with TRL Gas Conditioning Unit. The gases were then directed to another three way valve which can divert the gases to a feed stream connected to DSMS before entering the IGA chamber for determination of the feed composition. At this point, with the use of a three way valve (one inlet-two outlet), the current system configuration allows us to conduct experiments for two different pressure ranges: 0-1000 mbar pressure range and 0-5000 mbar pressure range. For the 0-1000 mbar pressure range experiments, the gas mixture was directly sent to the IGA chamber with a possibility of diverting the feed gas to a purge stream just before it enters the IGA, whereas for 0-5000 mbar pressure range experiments, the gas mixture were first sent to a back pressure regulator system consisting of a pressurized cylinder, back pressure regulator and manometer. The gasses which were sent at 7000 mbar from the gas flow regulators were directed to the pressurized cylinder connected to a manometer. Back pressure regulator enables to control the pressure of the gas mixture sent to the IGA chamber by purging the gas mixture above specified set point, and the pressurized cylinder, with its high volume, enables to prepare homogeneous gas mixtures. Outlet stream of the back pressure regulator system was then sent to the three way valve (two inlet-one outlet), which was connected to the stream used for the 0-1000 mbar range experiments, and sent to the IGA chamber with the same opportunity of diverting the feed gas to a purge stream just before it reaches the IGA unit.

Prepared adsorbent samples were weighted and placed in IGA chamber. The gasses, metered and mixed in the feed section, were sent to the IGA unit in which adsorption/desorption tests were conducted. There were two outlet streams from the chamber: the first one was directly sent to the DSMS for determination of unadsorbed gas amount (and concentrations), and the second one was sent to the vacuum pump. When the IGA chamber reached the set pressure value, automatic exhaust valve was opened and excess

gas was sent to the vacuum pump to control and stabilize the chamber pressure at the set point.

3.3. Adsorbent Preparation

Different oxidative, alkali and thermal treatments were used to prepare the activated carbon based adsorbents prepared and tested in this study.

A commercial activated carbon (Norit-ROX) was crushed and sieved to 45-60 mesh size (354-250 μm). This activated carbon material is called AC0. Then it was treated with 200 ml of 2 N HCl solution to remove some ash and sulfur content. Soxhlet apparatus was used for this treatment. 20-25 g of AC0 was placed in an extraction unit held by an extraction thimble. Extraction process was continued under total reflux for 12 hours. After the extraction process was completed, the slurry was rinsed with de-ionized water. In order to remove remaining HCl from the AC surface, the samples are washed again with de-ionized water for 6 hours. Finally, the slurry was dried at 115 °C overnight. This activated carbon material is referred to as AC1.

10-15 g of AC1 was oxidized in a down flow reactor under the flow of 10 ml/min O_2-190 ml/min N_2 (5% O_2-95% N_2) mixture for 10 hours at 450 °C. Heating up and cooling down processes were done under the flow of 150 ml/min N_2. The air oxidized AC material obtained through this procedure is called as AC2.

10-15 g of AC1 was put into a round bottom flask containing 350 ml of 5 N HNO_3 solution. This flask was heated up under total reflux for 3 hours. The suspension was allowed to precipitate through the night. The resulting precipitate was put in a 2 L beaker with 1.5 L de-ionized water. The mixture was boiled until 300 ml of water evaporated. The suspension was again allowed to precipitate through the night. The rinsing procedure was repeated until there was no precipitation (i.e. the solution had a homogeneous appearance). Then the solution was filtrated using vacuum filtration. Obtained AC was dried at 115 °C overnight. The HNO_3-oxidized AC material obtained through this procedure is called as AC3.

AC8 adsorbents were prepared by incipient-to-wetness impregnation technique described in Figure 3.1. AC2 was impregnated with 10% K_2CO_3 solution (2.1 ml deionized water/g AC) and subjected to calcination at different temperatures under flow of 5% O_2-95% N_2 mixture for 2 hours. The resulting adsorbents were named according to calcination temperatures as AC8-200, AC8-250 and AC8-300.

Similarly, AC3 samples were impregnated with 10% K_2CO_3 solution (2.1 ml deionized water/g AC) and subjected to calcination at different temperatures under flow of 5% O_2-95% N_2 mixture for 2 hours. The resulting adsorbents were named according to calcination temperatures as AC9-175, AC8-200 and AC9-250.

Table 3.3. List of activated carbon adsorbents.

Name	Treatment
AC0	NORIT ROX
AC1	HCl washed NORIT ROX
AC2	HCl washed and air oxidized NORIT ROX
AC3	HCl washed and HNO_3 oxidized NORIT ROX
AC8-200	K_2CO_3 impregnated and calcined (200 °C) AC2
AC8-250	K_2CO_3 impregnated and calcined (250 °C) AC2
AC8-300	K_2CO_3 impregnated and calcined (300 °C) AC2
AC9-175	K_2CO_3 impregnated and calcined (175 °C) AC3
AC9-200	K_2CO_3 impregnated and calcined (200 °C) AC3
AC9-250	K_2CO_3 impregnated and calcined (250 °C) AC3

3.4. Adsorption Tests

The CO_2 and CH_4 adsorption/desorption isotherms of activated carbon adsorbents were obtained by using the gravimetric system described in Section 3.2.3.

Pure CO_2 and pure CH_4 adsorption capacities; total adsorption capacity and selective adsorption capacities for each gas when a gas mixture was fed to the system, and

adsorption/desorption isotherms of the samples were obtained at each set pressure value in the range of 0-1000 mbar for three temperature values, i.e. room temperature (RT), 120 °C and 200 °C under the flow of pure CO_2 (50 ml/min CO_2), pure CH_4 (50 ml/min CH_4), 50% CO_2-50% CH_4 mixture (25 ml/min CO_2-25 ml/min CH_4), and 10% CO_2-90% CH_4 mixture (5 ml/min CO_2-45 ml/min CH_4), by IGA-DSMS.

In 0-5000 mbar pressure range experiments, adsorption/desorption isotherms, and selective and total adsorption capacities were obtained at each set pressure value for RT under the flow of pure CO_2 (50 ml/min CO_2), pure CH_4 (50 ml/min CH_4), 50% CO_2-50% CH_4 mixture (45 ml/min CO_2-45 ml/min CH_4), and 10% CO_2-90% CH_4 mixture (9 ml/min CO_2-81 ml/min CH_4).

In order to eliminate humidity and trapped gasses, 60-70 mg samples were outgassed at room temperature for overnight prior to the adsorption runs. In the adsorption tests conducted at 0-1000 mbar range, gas pressure was increased by 100 mbar in each step. For the high pressure tests, gas pressure was increased by 500 mbar in each step.

4. RESULTS AND DISCUSSION

The aim of the current work is to design and develop CO_2 adsorbents which can selectively adsorb CO_2 from a CO_2-CH_4 mixture. In this context, a commercial activated carbon, Norit ROX, was oxidized by air and HNO_3 oxidation, and two series of adsorbents, AC8 and AC9 series, respectively, were prepared on those oxidized ACs by K_2CO_3 impregnation following by calcination at various temperatures. SEM and EDX tests were performed on the prepared adsorbents in order to obtain information on their micro-structural properties. The CO_2 and CH_4 adsorption capacities of the samples under pure-gas feeds and selective adsorption performance of the samples under CO_2 + CH_4 mixed feed were studied by using IGA-DSMS system. Then adsorption on adsorbents was modelled, and the kinetics of CO_2 adsorption was studied.

The results of this study will be presented in three sections:

- Micro-characterization of the adsorbents
- Adsorption and selective adsorption studies
- Adsorption modelling and kinetic studies

4.1. Micro-characterization of the Adsorbents

In order to see the differences between the micro-structural properties of the K_2CO_3 impregnated samples prepared on air oxidized and nitric acid oxidized ACs, SEM-BSE (Back-Scattered composition image) of AC8-250 and AC9-250, which were prepared on air and HNO_3-oxidized AC respectively, are compared in Figure 4.1.

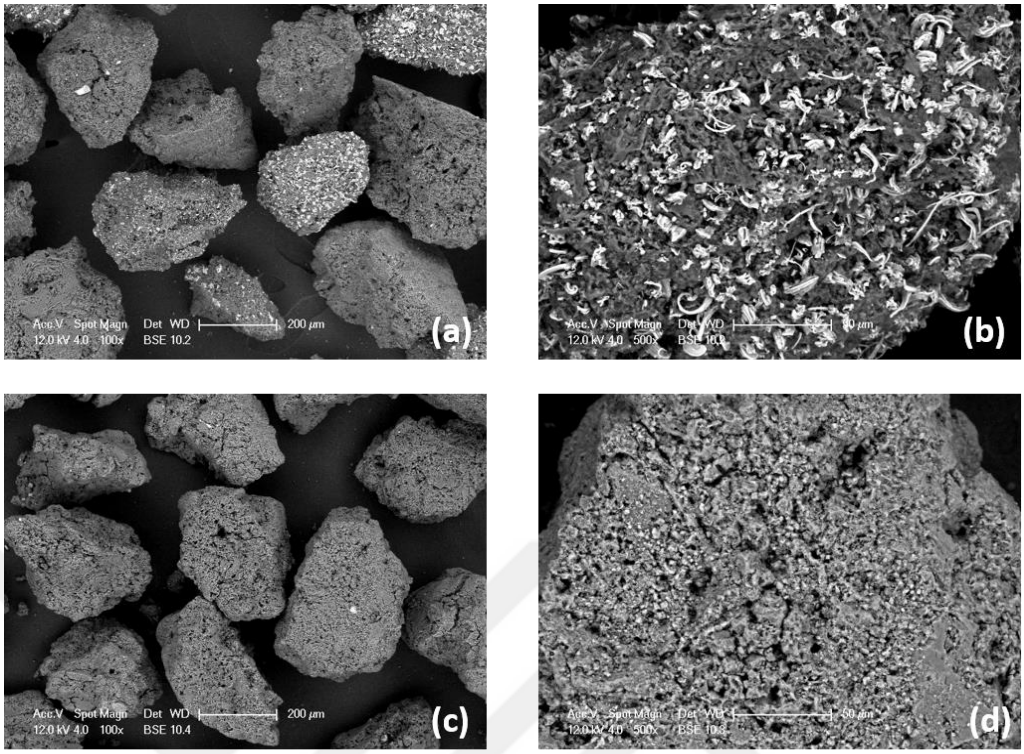

Figure 4.1. Back-scattered electrons micrographs of (a) AC8-250 (100x), (b) (500x) and (c) AC9-250 (100x), (d) (500x).

The analysis of the images reveal that the clusters formed on AC8-250 are not homogeneously distributed over the adsorbent, which was prepared by air oxidation followed by K_2CO_3 impregnation. In the area image, Figure 4.1-a, it is seen that some adsorbent particles have abundant amount of K crystals on their surface whereas others have smaller cluster formations and, thus, low amount of K on their surface. On the other hand, nitric acid oxidized and K_2CO_3 impregnated AC9-250 particles seemed to have similar surfaces with homogeneously dispersed K-formations having smaller size.

Figure 4.2 shows the SEM micrographs of AC8-250 and AC8-300, on which the final pretreatment, calcination, were conducted at 250 and 300 °C, respectively. A uniform distribution of K-formations was observed on the both samples prepared with 10% K_2CO_3 impregnation, and EDX results in general confirmed their surfaces have 5-7% K^+ on the average. The results also show that the exposed amount of K^+% increased with the increase in calcination temperature applied during the preparation of the adsorbent.

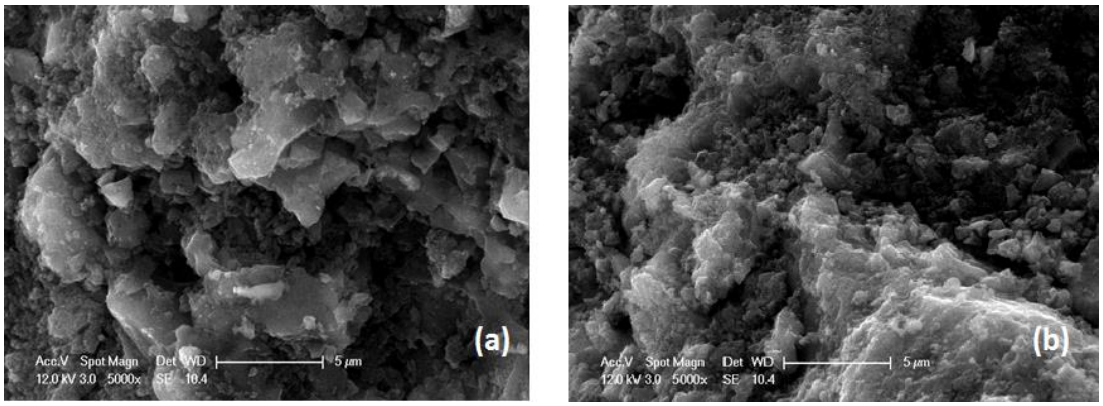

Figure 4.2. SEM micrographs of (a) AC8-250, (b) AC8-300 (x5000).

Back-scattered electrons micrographs of AC8-200, AC8-250, and AC8-300 adsorbents are given in Figure 4.3. Images show that AC8-300 had a more uniform K_2CO_3 distribution on its surface compared to that on AC8-200 and AC8-250 surfaces. The K agglomeration is evident on the surfaces of AC8-200 and AC8-250, as shown in Figures 4.3-a and 4.3-b.

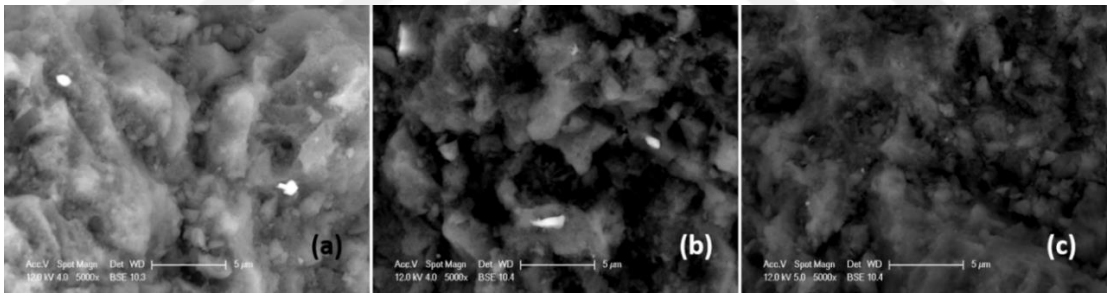

Figure 4.3. BSE images of (a) AC8-200, (b) AC8-250, and (c) AC8-300 (x5000).

Figure 4.4 shows the SEM micrographs and corresponding BSE images of nitric acid and K_2CO_3 impregnated AC9 series samples, AC9-175, AC9-200 and AC9-250, which were calcined at 175, 200 and 250 °C, respectively. A uniform distribution of K-formation was observed on the samples prepared with 10% K_2CO_3 impregnation; EDX results confirmed 8-9% K^+ surface concentration on the average. The results also indicate the calcination temperature does not significantly affect K^+ surface concentration.

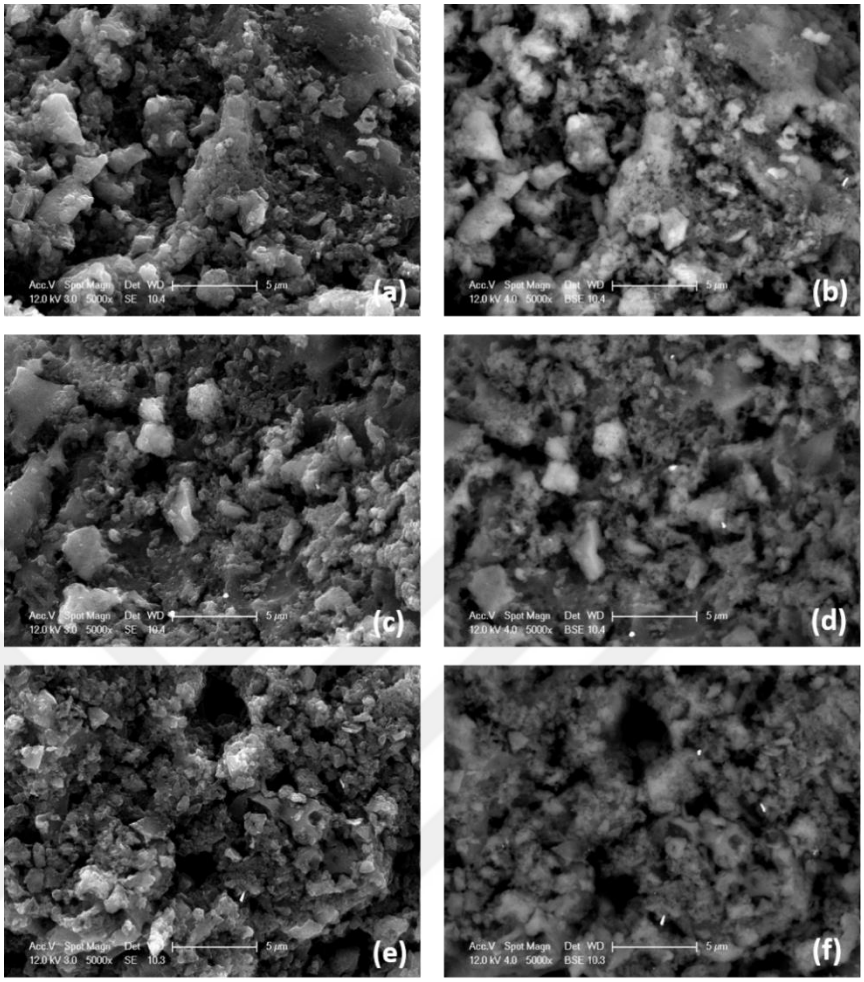

Figure 4.4. SEM images of (a) AC9-175, (c) AC9-200 , (e) AC9-250 and (b), (d), (f) corresponding BSE micrographs (x5000).

4.2. Adsorption and Selective Adsorption Studies

Adsorption/desorption and selective adsorption tests were conducted for 0-1000 mbar pressure range under 50 ml/min gas flow rate at RT, 120 °C and 200 °C for pure CO_2, pure CH_4 and their mixtures, 50% CO_2-50% CH_4 and 10% CO_2-90% CH_4.

High pressure adsorption tests were conducted for 0-5000 mbar pressure range at RT under 50 ml/min and 90 ml/min gas flow rates for pure gas and gas mixture tests, respectively.

4.2.1. Adsorption/Desorption Test Results for 0-1000 mbar Pressure Range Experiments

This section presents the results of the adsorption and selective adsorption tests conducted for the pure gas and gas mixture feeds, respectively, for 0-1000 mbar pressure range.

4.2.1.1. Adsorption/Desorption Studies Under Pure 50 ml/min CO_2 and Pure 50 ml/min CH_4 Flow Rates.

The adsorption isotherms obtained for AC8-200 sample under pure 50 ml/min CO_2 flow and pure 50 ml/min CH_4 flow are given in Figure 4.5 and Figure 4.6, respectively. At RT and 1000 mbar pressure, the mass uptake for pure CO_2 adsorption was measured as 10.21%, while the mass uptake for CH_4 adsorption only reached the value of 1.48%. The results of the pure gas adsorption tests conducted on AC8-200 samples showed that CO_2 mass uptake of the adsorbent at 1000 mbar and RT is 6.9 times higher than CH_4 mass uptake for the same conditions.

The results clearly showed that CO_2 and CH_4 adsorption capacity of the samples decreases significantly with the increase in adsorption temperature.

Figure 4.7. and 4.8. show the mass uptake values of AC8-250 sample under pure 50 ml/min CO_2 flow and pure 50 ml/min CH_4 flow, respectively. At 1000 mbar and RT, the mass uptake of the sample was determined as 9.5% for pure CO_2 adsorption, whereas the mass uptake for CH_4 adsorption was found as 1.2%, revealing CO_2 adsorption capacity of the AC8-250 is 7.9 times greater than its CH_4 adsorption capacity for the same conditions.

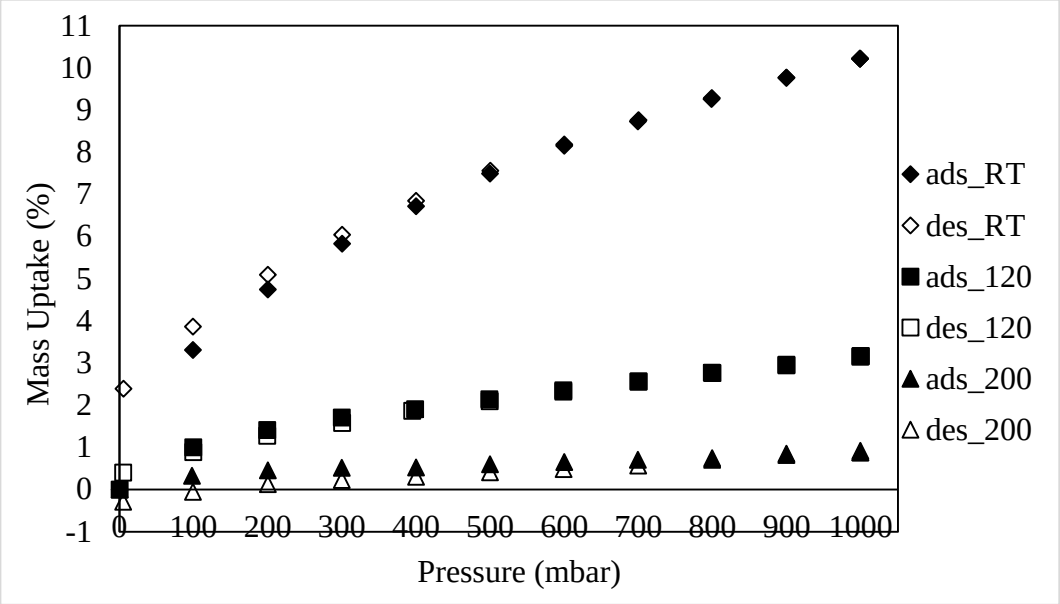

Figure 4.5. The mass uptake of AC8-200 sample under 50 ml/min CO_2 flow.

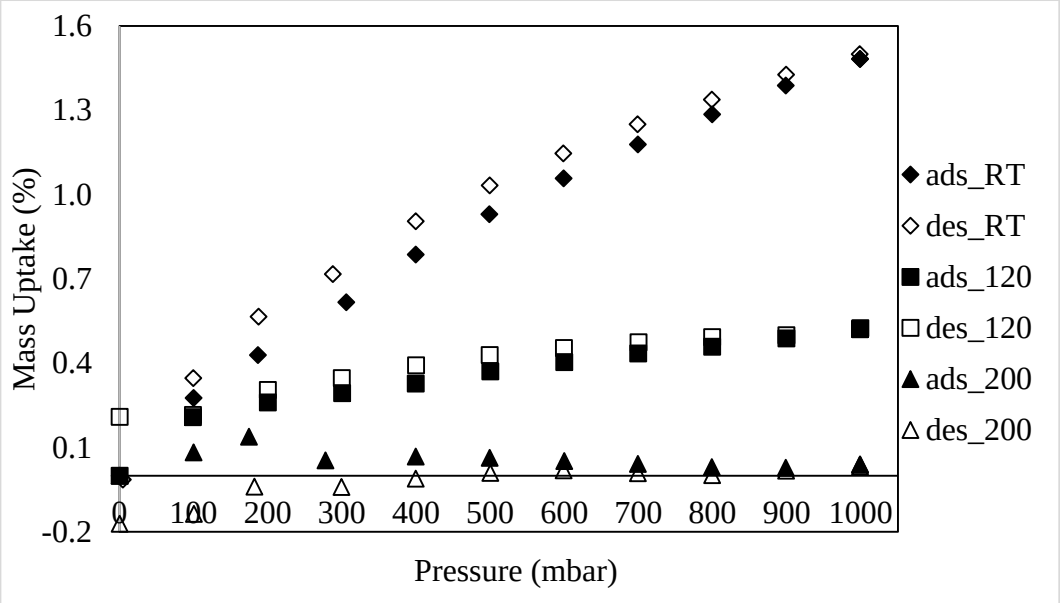

Figure 4.6. The mass uptake of AC8-200 sample under 50 ml/min CH_4 flow.

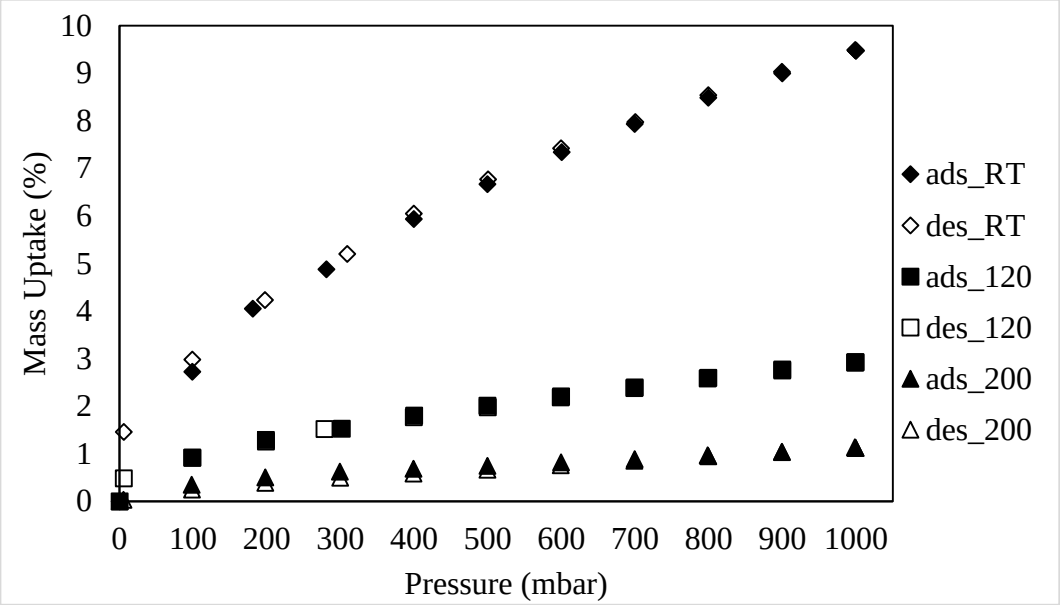

Figure 4.7. The mass uptake of AC8-250 sample under 50 ml/min CO_2 flow.

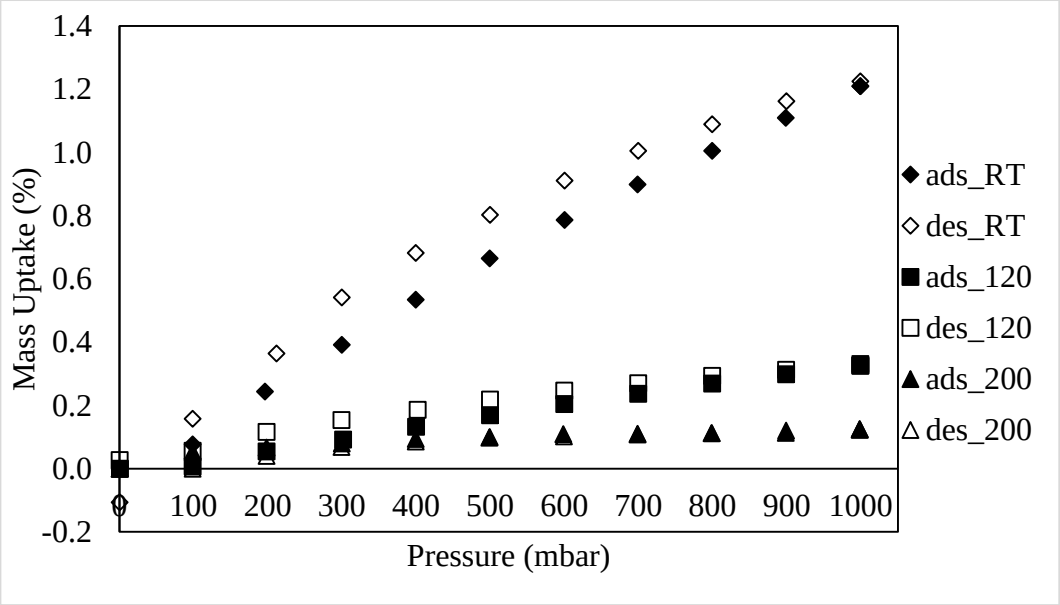

Figure 4.8. The mass uptake of AC8-250 sample under 50 ml/min CH_4 flow.

The results of the adsorption/desorption tests conducted on AC8-300 samples at different temperatures under pure 50 ml/min CO_2 flow and pure 50 ml/min CH_4 flow are shown in Figure 4.9 and 4.10, respectively.

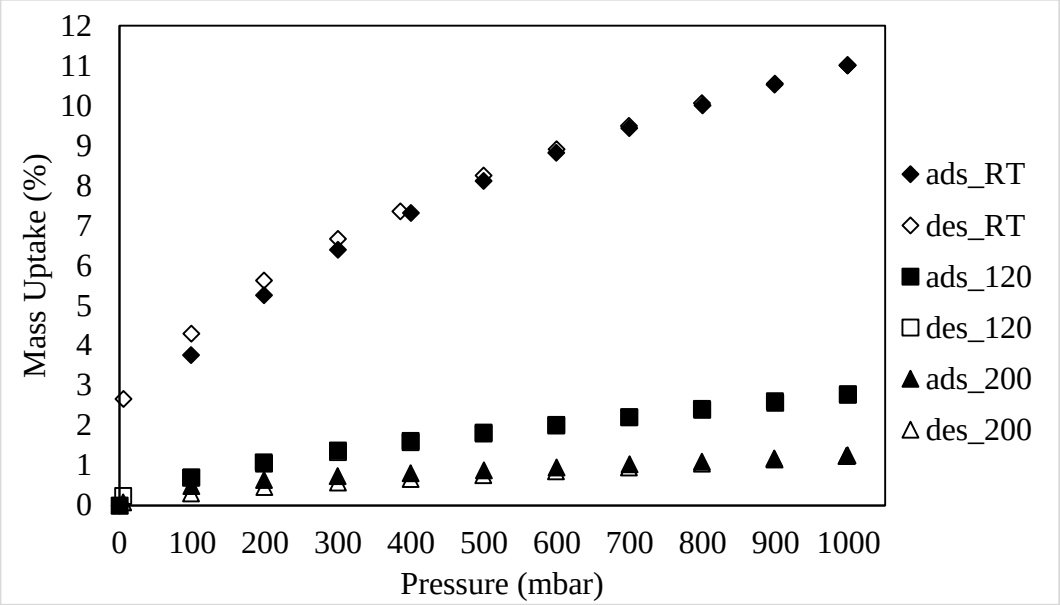

Figure 4.9. The mass uptake of AC8-300 sample under 50 ml/min CO_2 flow.

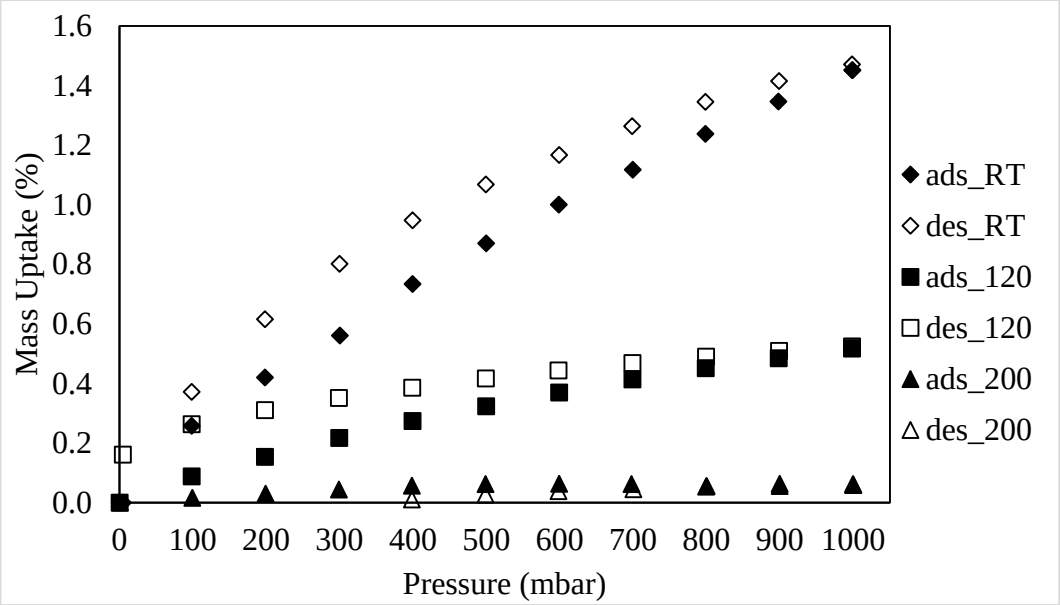

Figure 4.10. The mass uptake of AC8-300 sample under 50 ml/min CH_4 flow.

At 1000 mbar and RT, AC8-300 reached the highest CO_2 and CH_4 adsorption capacities as 11% and 1.45%, respectively. The results of the pure gas tests show that CO_2 adsorption capacity of AC8-300 is 7.6 times higher than its CH_4 adsorption capacity under the same conditions.

The adsorption/desorption mass uptake profiles obtained for AC9-200 at different temperatures under pure CO_2 and pure CH_4 flows are presented in Figure 4.11 and Figure 4.12, respectively. At RT, 7.3% mass uptake was observed for pure CO_2 adsorption, whereas the mass uptake for CH_4 adsorption only reached 0.8%. Tests conducted on AC9-200 samples with pure gasses showed that CO_2 mass uptake of the adsorbent at 1000 mbar and RT is 6.9 times higher than CH_4 mass uptake.

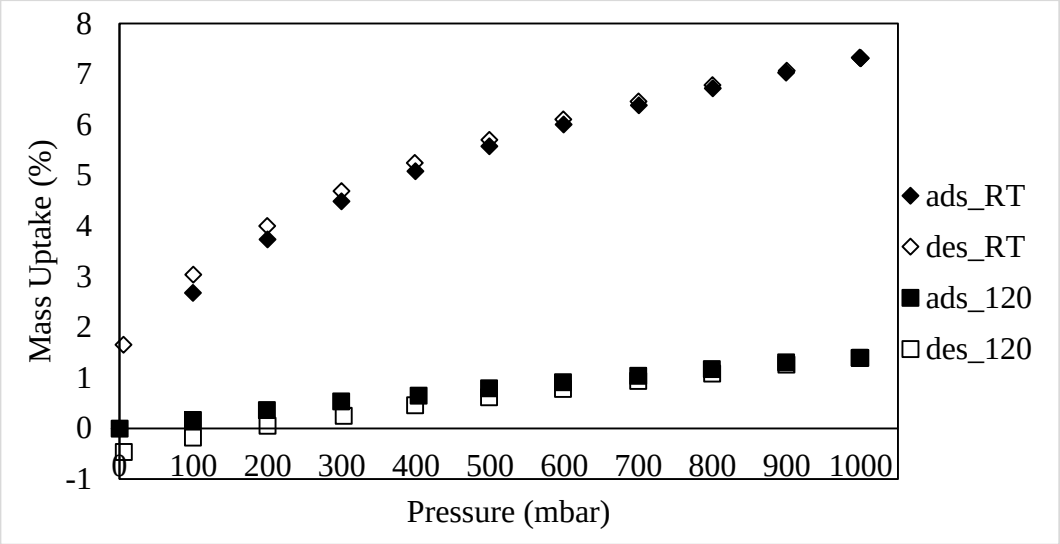

Figure 4.11. The mass uptake of AC9-200 sample under 50 ml/min CO_2 flow.

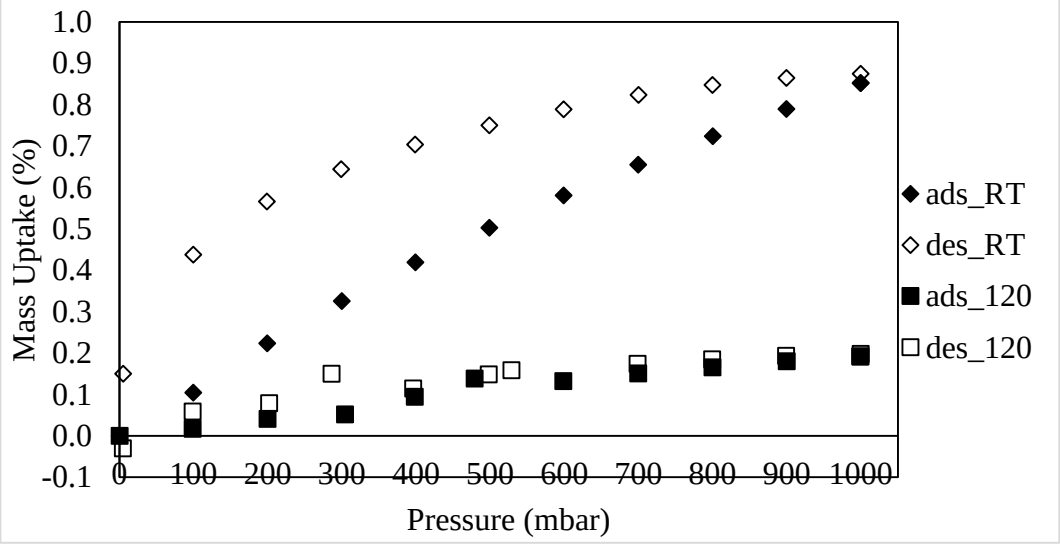

Figure 4.12. The mass uptake of AC9-200 sample under 50 ml/min CH_4 flow.

When the effect of temperature on adsorption behavior is analyzed, it is seen that adsorbed amount of both CO_2 and CH_4 decreases with the increase in temperature. In desorption process, temperature was leading just the opposite trend; at high temperature desorption occurred more easily than it did at RT.

The properties of the K_2CO_3 impregnated adsorbents are directly related with the type of oxidation applied to the AC support and the calcination temperature. In order to see the effect of oxidation type, the adsorption behaviors of AC8-200 (air oxidation) and AC9-200 (HNO_3 oxidation) samples are compared, in terms of their mass uptake values, under pure CO_2 and pure CH_4 feeds in Figure 4.13.

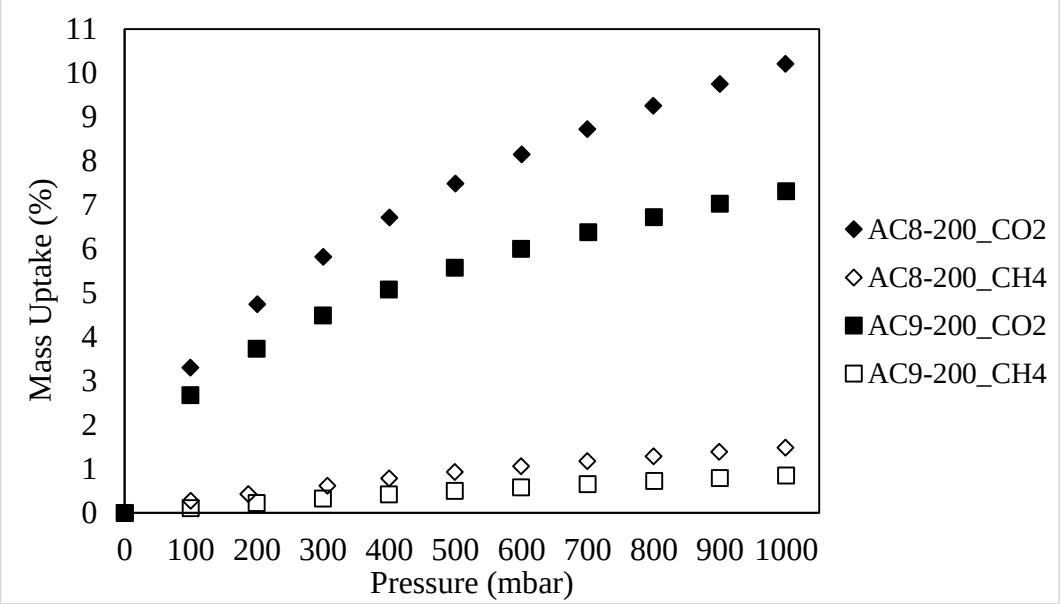

Figure 4.13. The comparison of AC8-200 and AC9-200 samples for mass uptake values under 50 ml/min CO_2 and 50 ml/min CH_4 flows.

The mass uptake values presented at Figure 4.13. show that although AC8-200 had captured a higher amount of CO_2, adsorbed CO_2/CH_4 weight ratio was higher for AC9-200 sample.

In order to see the effect of calcination temperature, adsorption behaviors of AC8-200, AC8-250 and AC8-300 samples are compared, in terms of their adsorption/desorption isotherm profiles, under pure CO_2 and pure CH_4 feeds. In the experiments conducted at 200

°C, AC8-200 and AC8-250 samples weighed less at the end of the adsorption/desorption cycles compared to their original weight. Therefore, their mass uptake values were calculated as below 0% at the end of the experiments. This can be seen from Figures 4.5-8. The main reason for that is most probably the loss of the oxygen bearing surface groups present on their surface due to high temperature, indicating the surfaces of AC8-200 and A8-250 samples are not very stable at elevated adsorption temperatures. AC8-300 sample, on the other hand, did not lose its surface groups at high adsorption temperatures (Figure 4.9-10). Since the only difference between these three samples is the calcination temperature applied, it can be said that the higher the calcination temperature, the more stable the surfaces become.

The adsorbed amounts of CO_2 and CH_4 under pure CO_2 and pure CH_4 feeds at 1000 mbar and RT for all AC8 and AC9 series samples are given in Figure 4.14 as mass uptakes. AC9 adsorbents showed significantly lower CO_2 and CH_4 adsorption capacities than those of AC8's. The highest CO_2 adsorption capacity was observed for AC8-300 sample, while it exhibited similar CH_4 adsorption capacity to AC8-200. CO_2 adsorption is confirmed to be reversible on all samples as there is no significant deviation observed between their adsorption and desorption profiles, whereas partial irreversibility was observed for CH_4 adsorption.

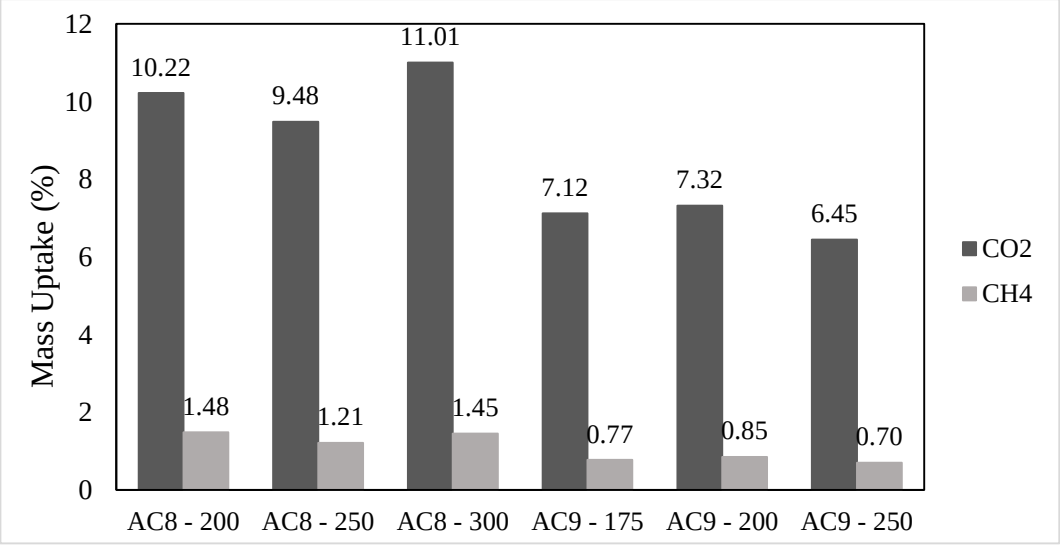

Figure 4.14. The mass uptake values for all samples at 1000 mbar and RT under 50 ml/min CO_2 and 50 ml/min CH_4 flows.

4.2.1.2. Selective Adsorption/Desorption Studies Under 50 ml/min Total Flow.

The CO_2 and CH_4 mass uptake values obtained for AC8-200 under 25 ml/min CO_2-25 ml/min CH_4 (50% CO_2-50% CH_4) flow are given, as mg/g adsorbent, in Figure 4.15 and Figure 4.16, respectively. Figures 4.17 and 4.18 show the CO_2 and CH_4 mass uptake values for the same sample under 5 ml/min CO_2-45 ml/min CH_4 (10% CO_2-90% CH_4) flow. Calculations performed for adsorption tests conducted under CO_2 + CH_4 feeds with different compositions revealed that CO_2 adsorption is more responsive to temperature; under 25 ml/min CO_2-25 ml/min CH_4 flow, adsorbed CO_2 amount at 1000 mbar and RT was found to be 47 mg/g adsorbent, while it decreased down to 16.6 mg/g at 120 °C, and to 4.9 mg/g at 200 °C, which was nearly 10% of the adsorbed amount at RT (Figure 4.15). The adsorbed CH_4 amount also decreased with increasing temperature (Figure 4.16 and Figure 4.18). However, the decrease in the adsorbed CH_4 amount was not as drastic as the decrease in the adsorbed CO_2 amount. Under 25 ml/min CO_2-25 ml/min CH_4 flow, adsorbed CH_4 amount at 1000 mbar and RT was found as 13 mg/g adsorbent, whereas at 200 °C it decreased down to 2.2 mg/g, which was nearly 20% of the amount of adsorbed CH_4 at RT.

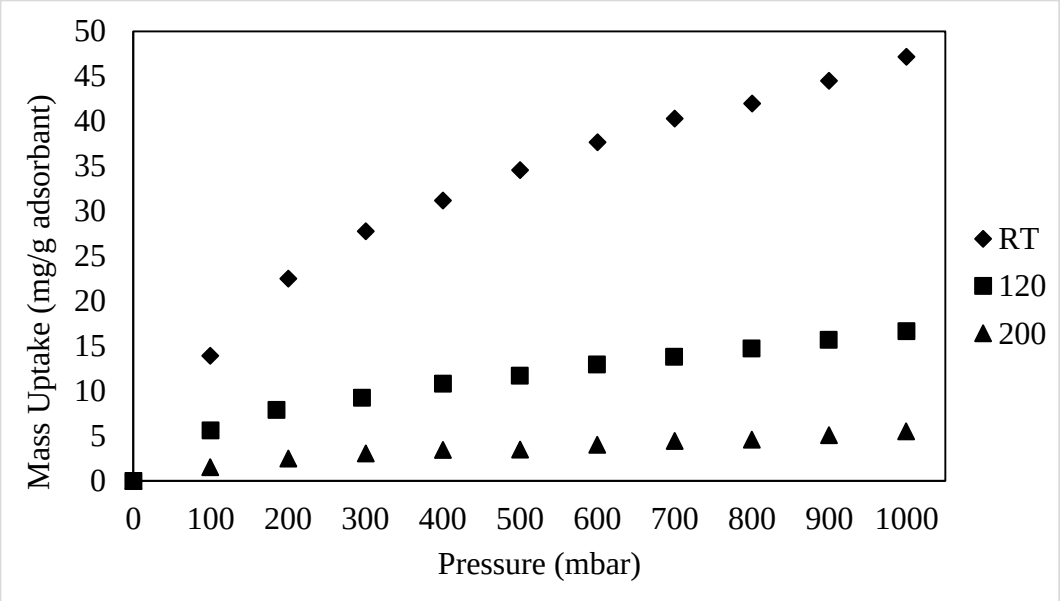

Figure 4.15. The adsorbed CO_2 amounts of AC8-200 under 25 ml/min CO_2-25 ml/min CH_4 flow.

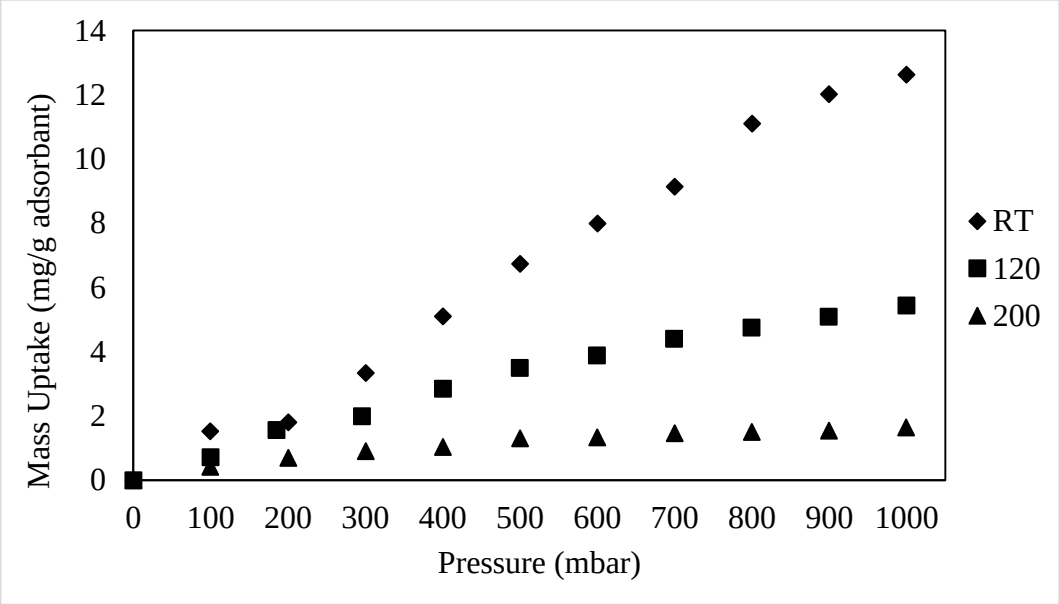

Figure 4.16. The adsorbed CH_4 amounts of AC8-200 under 25 ml/min CO_2-25 ml/min CH_4 flow.

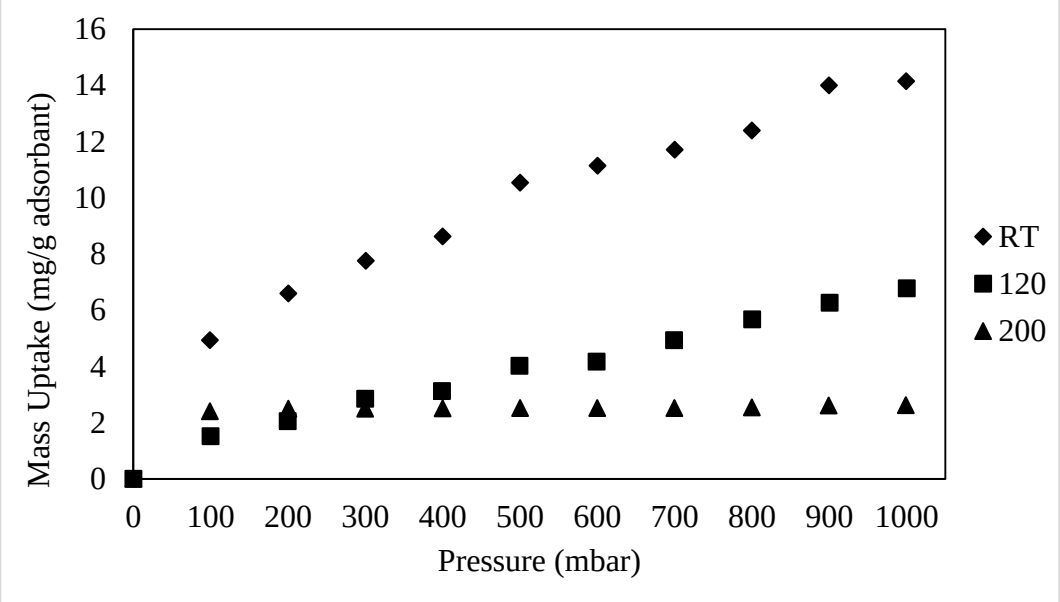

Figure 4.17. The adsorbed CO_2 amounts of AC8-200 under 5 ml/min CO_2-45 ml/min CH_4 flow.

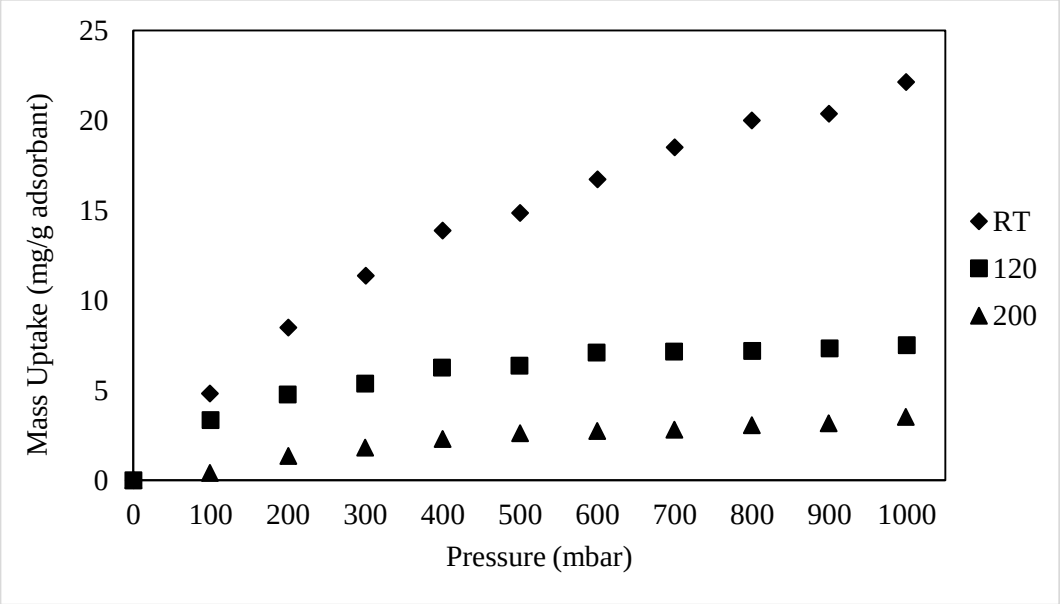

Figure 4.18. The adsorbed CH_4 amounts of AC8-200 under 5 ml/min CO_2-45 ml/min CH_4 flow.

The effect of the CO_2 concentration in the gas mixture fed on the total (i.e. CO_2 + CH_4) amount absorbed on AC8-200 as percentage of mass uptake is given as an example in Figure 4.18.

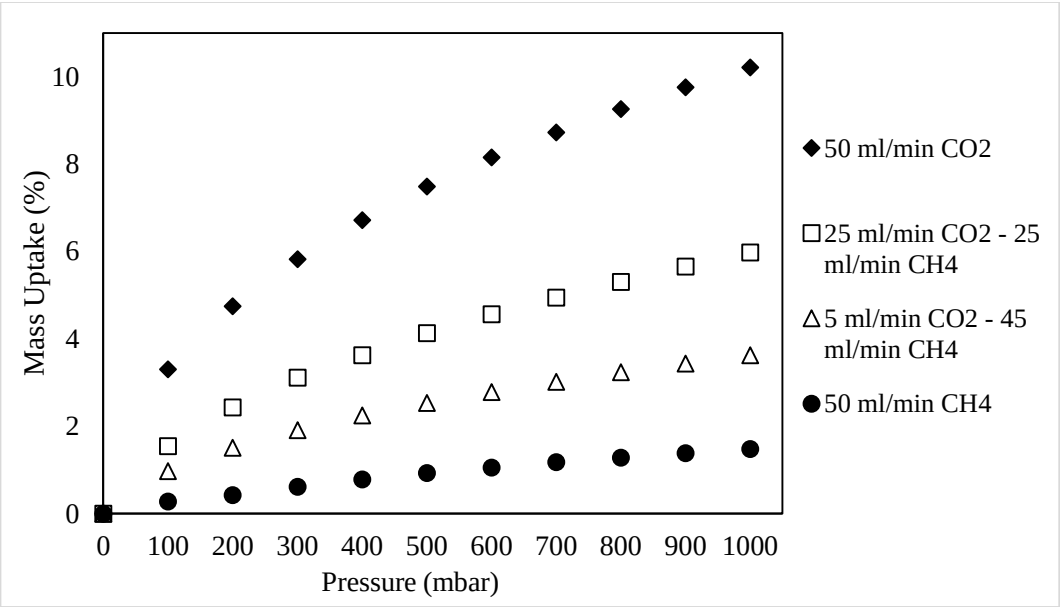

Figure 4.19. The mass uptakes of AC8-200 under different flow compositions.

The total CO_2 + CH_4 adsorption on AC8-200, as mass uptake percentage, were 10.2 wt.% under pure 50 ml/min CO_2 flow, 6 wt.% under 25 ml/min CO_2-25 ml/min CH_4 flow, 3.6 wt.% under 5 ml/min CO_2-45 ml/min CH_4 flow, and 1.5% under 50 ml/min CH_4 flow (Figure 4.19). These results indicated that as the CH_4 concentration in the CO_2 + CH_4 mixture feed increases, total adsorbed amount decreases. In order to investigate the reason for this decrease further, the change in adsorbed CO_2 and CH_4 amounts with pressure under 25 ml/min CO_2-25 ml/min CH_4 flow are presented in Figure 4.20. In the total amount adsorbed, which was 59.7 mg/g, adsorbed CO_2 and CH_4 amounts were calculated as 47.1 mg/g and 12.6 mg/g, respectively, clearly shows the adsorbent AC8-200 selectively adsorbs CO_2. In terms of mass, when CO_2:CH_4 ratio in the gas mixture fed was 2.75, the mass ratio CO_2:CH_4, in the total amount adsorbed was found as 3.7.

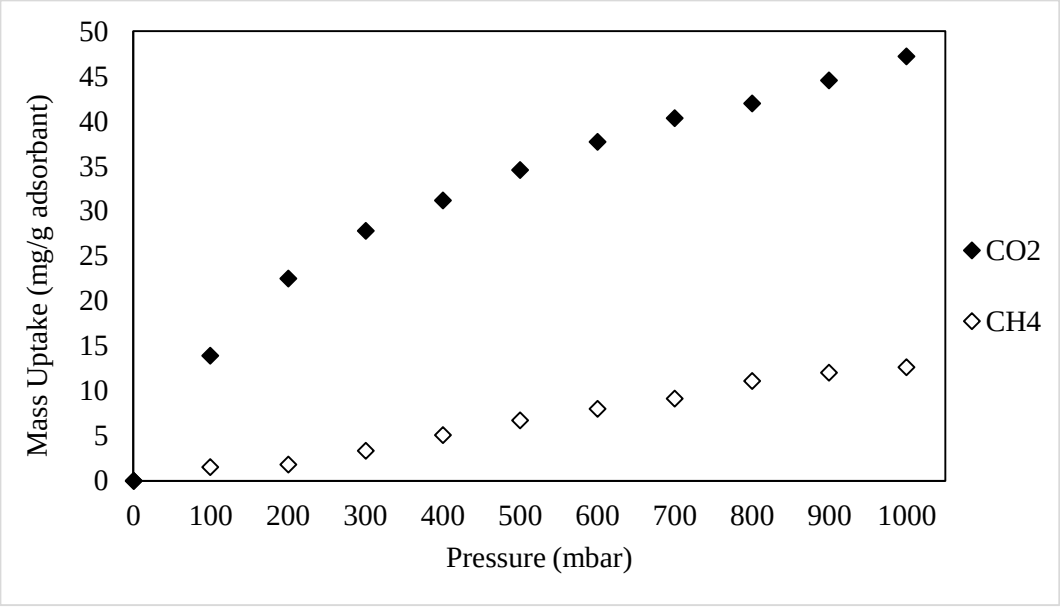

Figure 4.20. The adsorbed amounts of CO_2 and CH_4 on AC8-200 under 25 ml/min CO_2-25 ml/min CH_4 flow at RT.

The change of CO_2:CH_4 ratio according to pressure is given in Figure 4.21.

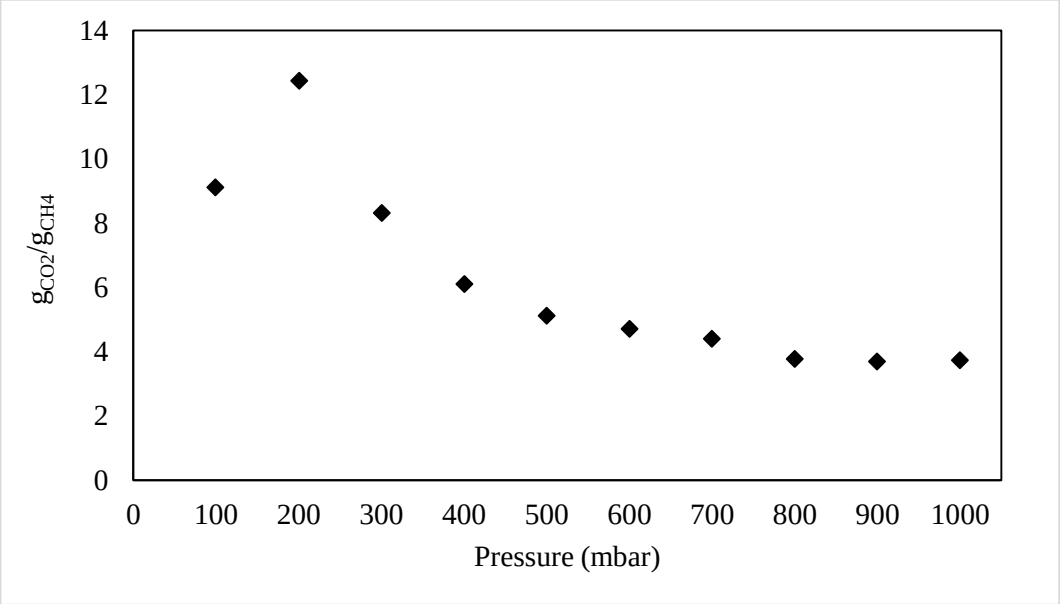

Figure 4.21. The adsorbed CO_2:CH_4 ratio on AC8-200 under 25 ml/min CO_2-25 ml/min CH_4 flow at RT.

The change in the adsorbed CO_2 and CH_4 amounts on AC8-200 at RT under 5 ml/min CO_2-45 ml/min CH_4 flow as a function of pressure is presented in Figure 4.22. In the total 36 mg/g adsorption, shares of CO_2 and CH_4 were calculated as 14 mg/g and 22 mg/g, respectively. The weight-based CO_2:CH_4 ratio in the feed was 0.3, while the adsorbed CO_2:CH_4 ratio was found as 0.6. The results reveal that as the weight-based CO_2:CH_4 feed ratio was decreased from 2.75 to 0.3, the ratio of CO_2:CH_4 in the adsorbed state was decreased from 3.7 to 0.6. The change in the CO_2:CH_4 adsorption ratio in response to pressure for AC8-200 sample at RT under 5 ml/min CO_2 - 45 ml/min CH_4 flow is given in Figure 4.23.

As it can be seen from Figure 4.23, CO_2:CH_4 adsorption ratio decreases with the increase in pressure up to 400 mbar, and stay constant at that level, ca. 0.65, in 400-1000 mbar total pressure range.

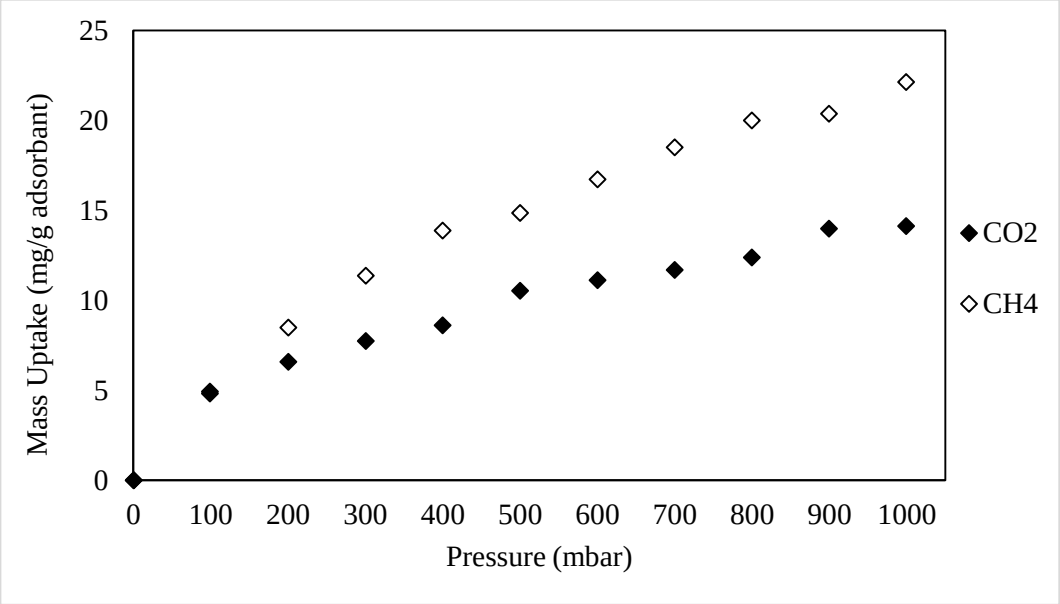

Figure 4.22. The adsorbed amounts of CO_2 and CH_4 on AC8-200 under 5 ml/min CO_2-45 ml/min CH_4 flow at RT.

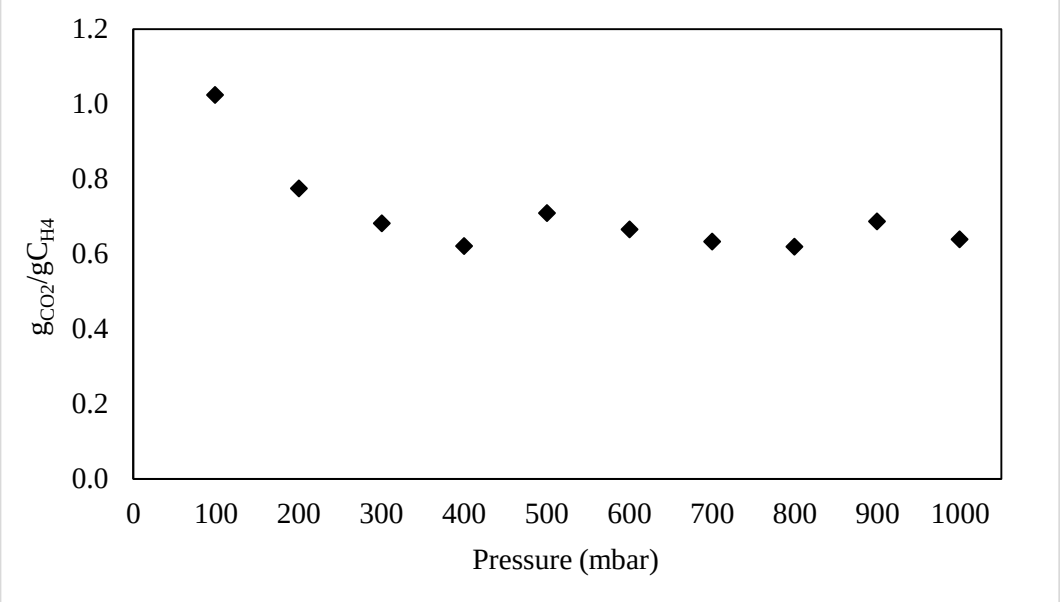

Figure 4.23. The adsorbed CO_2:CH_4 ratio on AC8-200 under 5 ml/min CO_2-45 ml/min CH_4 flow at RT.

In order to compare selective adsorption performances of all K_2CO_3 impregnated adsorbents prepared in the current study, the results of the adsorption tests conducted at RT

under 50% CO_2-50% CH_4 and under 10% CO_2-90% CH_4 (by volume) gas mixture feeds are comparatively presented in Figure 4.24 and Figure 4.25, respectively.

The highest total adsorption (CO_2 + CH_4) was observed on AC8-300. Although AC8-250 has the highest CO_2 adsorption for the 50% CO_2-50% CH_4 feed gas mixture, CO_2:CH_4 adsorption selectivity ratio was at its highest on AC8-200 reading the value 3.7. (Figure 4.24). The adsorption/selective adsorption performance of the samples prepared on HNO_3 oxidized AC, AC9s, were found inferior compared to the performance of the samples prepared on air oxidized AC, AC8s. Though the adsorbed CO_2 amounts on AC8-200, AC8-250, and AC8-300 were very close to each other, AC8-300 had the highest CH_4 adsorption (Figure 4.24).

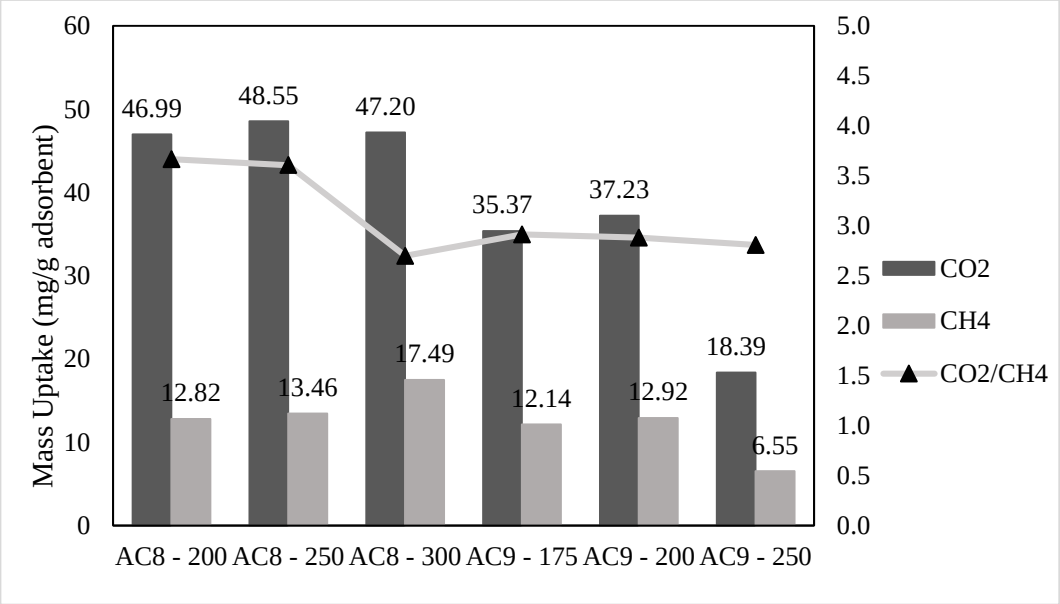

Figure 4.24. The CO_2 and CH_4 mass uptake values for all samples at 1000 mbar and RT under 25 ml/min CO_2-25 ml/min CH_4 flow.

The results obtained from the tests conducted under 5 ml/min CO_2-45 ml/min CH_4 flow (i.e. 10% CO_2-90% CH_4) at RT, both the highest total (CO_2 + CH_4) adsorption and the highest CO_2 adsorption were observed on AC8-300. As AC8-300 sample also had the highest CH_4 adsorption, its selective adsorption performance was rather limited. AC8-250 reached the highest CO_2:CH_4 selectivity ratio, though the amount of CO_2 adsorbed on it is less than that on AC8-300 (Figure 4.25).

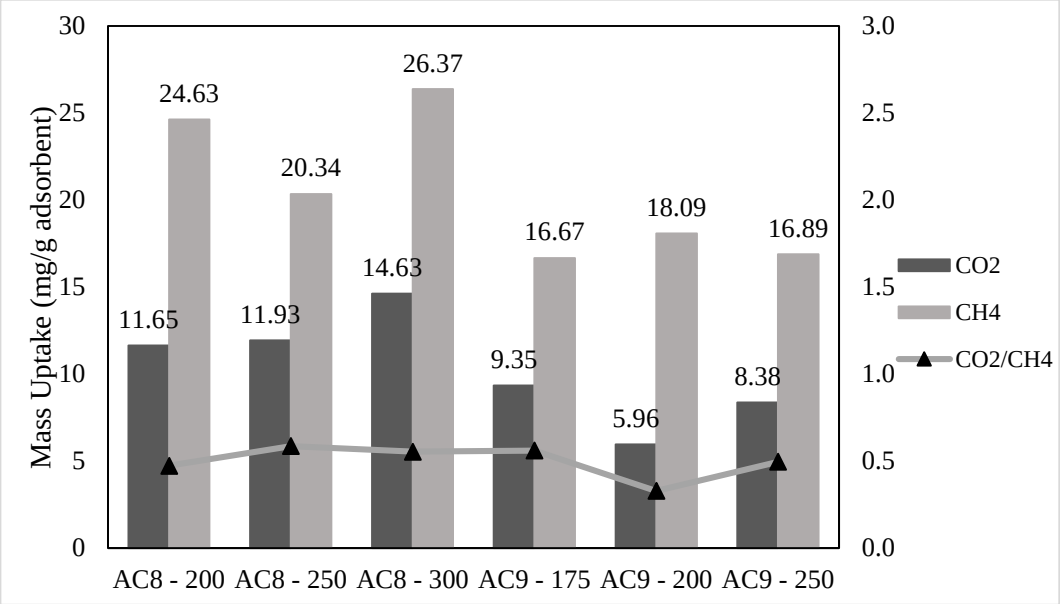

Figure 4.25. The CO_2 and CH_4 mass uptake values for all samples at 1000 mbar and RT under 5 ml/min CO_2-45 ml/min CH_4 flow.

4.2.2. High Pressure Adsorption/Desorption and Selective Adsorption Studies for 0-5000 mbar Pressure Range

The adsorption/desorption and selective adsorption tests for 0-5000 mbar (total) pressure range were performed on AC-200, which has the highest selectivity towards CO_2 adsorption in the tests conducted at RT for 0-1000 mbar pressure range. The effect of the CO_2 amount in the feed gas mixture on total adsorption capacity is presented in Figure 4.26. The total CO_2 + CH_4 adsorption on the AC8-200 sample were 19.7 wt.% under 50 ml/min CO_2 flow, 13.5 wt.% under 45 ml/min CO_2-45 ml/min CH_4 flow, 7.6 wt.% under 9 ml/min CO_2-81 ml/min CH_4 flow, and 3.9 wt.% under 50 ml/min CH_4 flow (Figure 4.26). These results are parallel to what had been observed in the tests conducted in 0-1000 mbar pressure range that as CH_4 amount in the gas mixture increases, total (CO_2 + CH_4) amount adsorbed decreases.

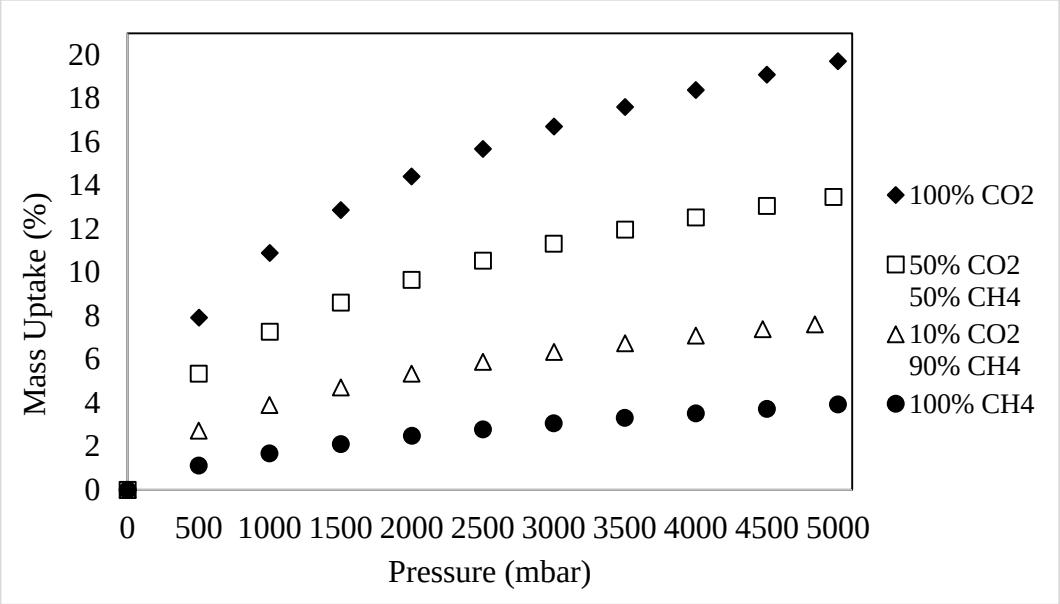

Figure 4.26. The mass uptakes of AC8-200 under different flow compositions.

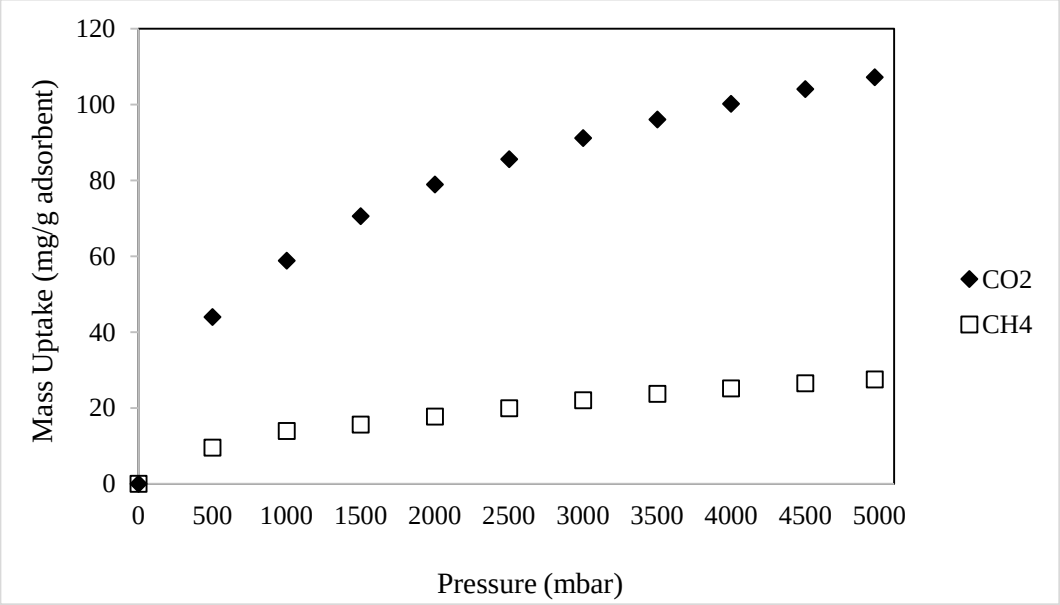

Figure 4.27. The adsorbed amounts of CO_2 and CH_4 on AC8-200 under 45 ml/min CO_2 - 45 ml/min CH_4 flow at RT.

In Figure 4.27, the change in the adsorbed amounts of CO_2 and CH_4 as a function of pressure under 45 ml/min CO_2-45 ml/min CH_4 flow is presented. The contribution of CO_2 adsorption to the total amount adsorbed, 134.8 mg/g, was calculated as 107.23 mg/g, limiting

CH_4 adsorption to 27.5 mg/g. As the mass based adsorption selectivity ratio CO_2:CH_4 on AC8-200 is 3.8 at RT for 0-5000 mbar total pressure and this value is significantly greater than CO_2:CH_4 ratio in the feed gas, 2.75; it is clear that AC8-200 is an adsorbent having selectivity towards CO_2. The change in adsorption selectivity ratio CO_2:CH_4 as a function of total pressure is given in Figure 4.29.

The change in the amounts of adsorbed CO_2 and CH_4 on AC8-200 as a function of pressure at RT under 9 ml/min CO_2-81 ml/min CH_4 flow is presented in Figure 4.28. The total adsorption at 5000 mbar was measured by IGA as 76.2 mg/g, and combined IGA-MS analysis revealed that the adsorbed amounts of CO_2 and CH_4 are 23.9 mg/g and 52.3 mg/g, respectively. The results confirm the selectivity of AC8-200 towards CO_2 as the mass based adsorption selectivity ratio, which was calculated as 0.5, is significantly greater than CO_2:CH_4 feed ratio, which is 0.3. In response to the decrease in CO_2:CH_4 feed ratio from 2.75 to 0.3, the adsorption selectivity ratio decreases from 3.89 to 0.5. The change in adsorption selectivity of AC8-200 as a function of total pressure at RT under 9 ml/min CO_2-81 ml/min CH_4 feed flow is given in Figure 4.29.

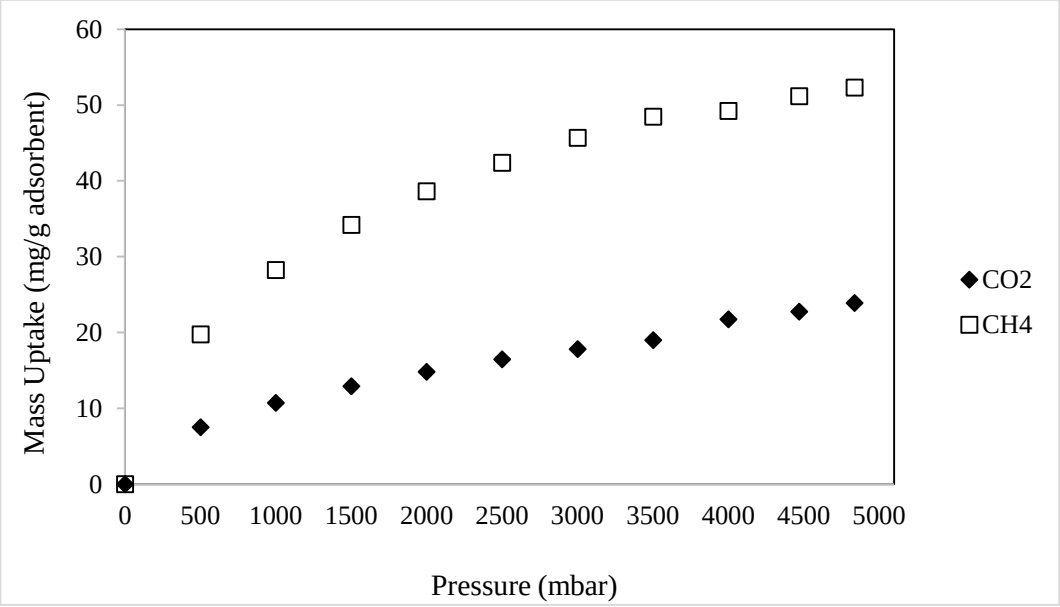

Figure 4.28. The adsorbed amounts of CO_2 and CH_4 on AC8-200 under 9 ml/min CO_2-81 ml/min CH_4 flow at RT.

The results clearly show that the mass ratio based CO_2:CH_4 adsorption selectivity ratio slightly fluctuates till 2000 mbar and then makes a plateau with the increase in pressure at ca. 4 (Figure 4.29)

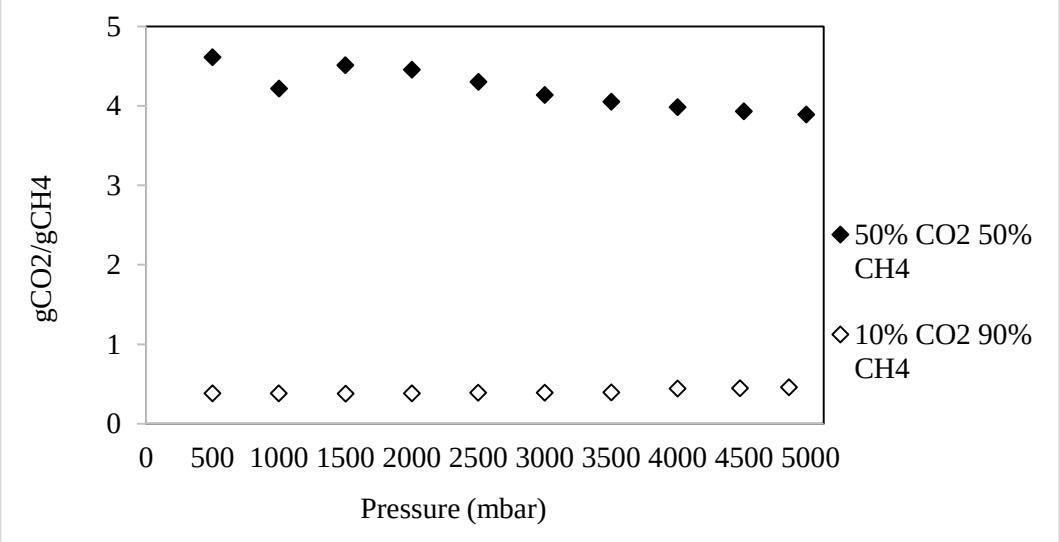

Figure 4.29. The adsorbed CO_2:CH_4 ratio on AC8-200 under 45 ml/min CO_2-45 ml/min CH_4 and under 9 ml/min CO_2-81 ml/min CH_4 flows at RT.

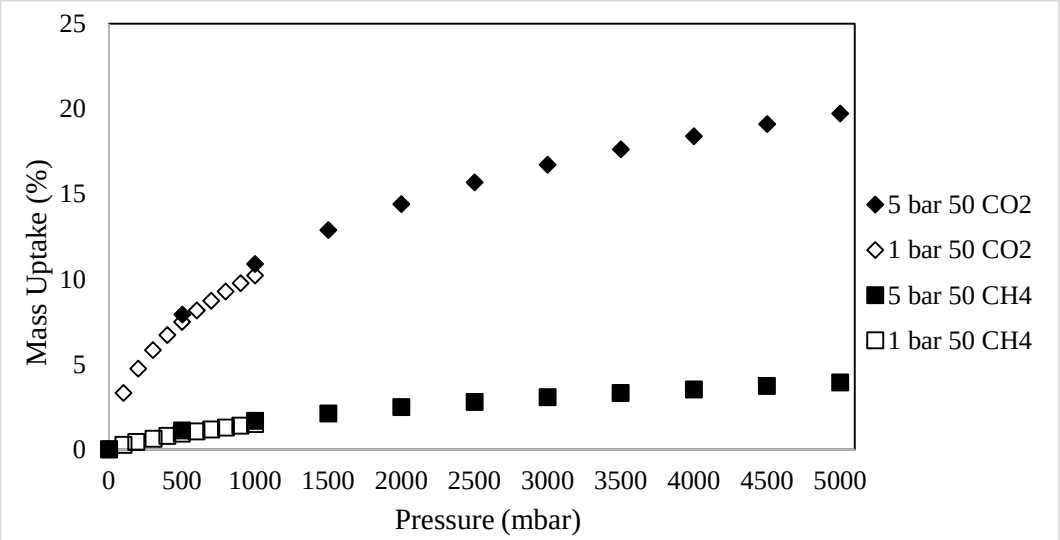

Figure 4.30. The mass uptake of AC8-200 sample under 50 ml/min CO_2 and under 50 ml/min CH_4 flows for experiments conducted for 0-1000 pressure range and 0-5000 mbar pressure range.

A clear match between mass uptake trends obtained for pure gas feeds in 0-1000 mbar and 0-5000 mbar pressure ranges clearly shows the reliability of the adsorption measurements (Figure 4.30).

4.3. Adsorption Modelling and Kinetic Studies

4.3.1. Adsorption Modelling

The experimental adsorption isotherm data, which were obtained for three temperature values, i.e. RT, 120 °C and 200 °C, between 0-1000 mbar pressure range were fitted to Langmuir, Freundlich and Dubinin-Radushkevich (D-R) models to describe the adsorption characteristics of the designed and prepared adsorbents. The graphs with experimental adsorption data for AC8-250 sample are given as examples to Freundlich (log(Q) vs. log(P)) and Dubinin Radushkevich (ln(W) vs. $(\ln(P_{sat}/P))^2$) isotherm models (Figures 4.31-34). According to correlation analysis results, Freundlich and D-R models are more successful in explaining CO_2 and CH_4 adsorption behaviors of AC samples. As it was expected, Langmuir isotherm model, which is based on the monolayer adsorption assumption, was not good at explaining the adsorption behaviors of ACs. The adsorption parameters calculated according to all three adsorption models are given in Tables 4.4-9.

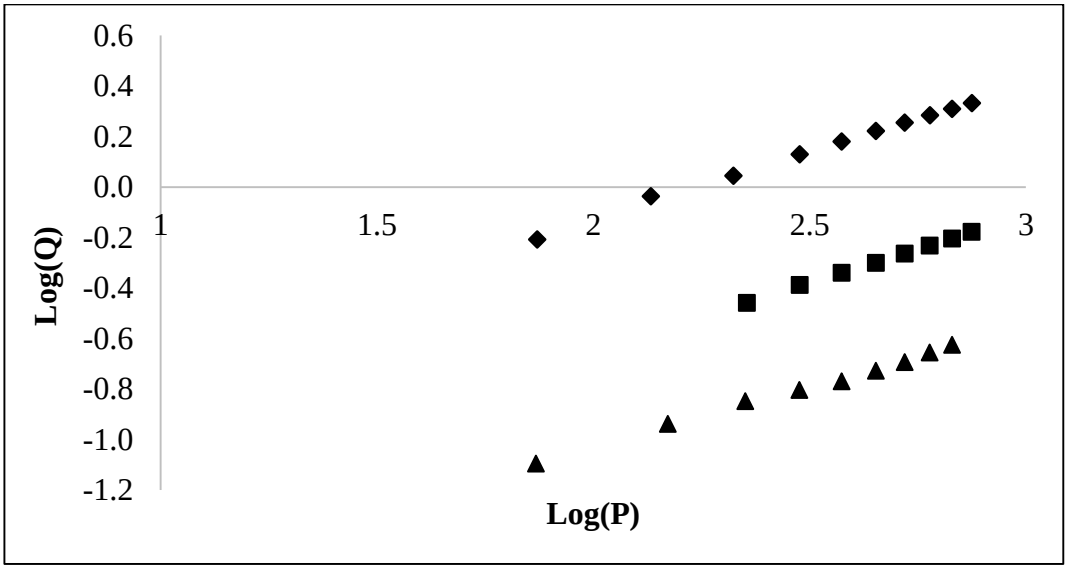

Figure 4.31. Freundlich Isotherms of CO_2 adsorption on A8-250 (♦) 25 °C, (■) 120 °C and (▲) 200 °C.

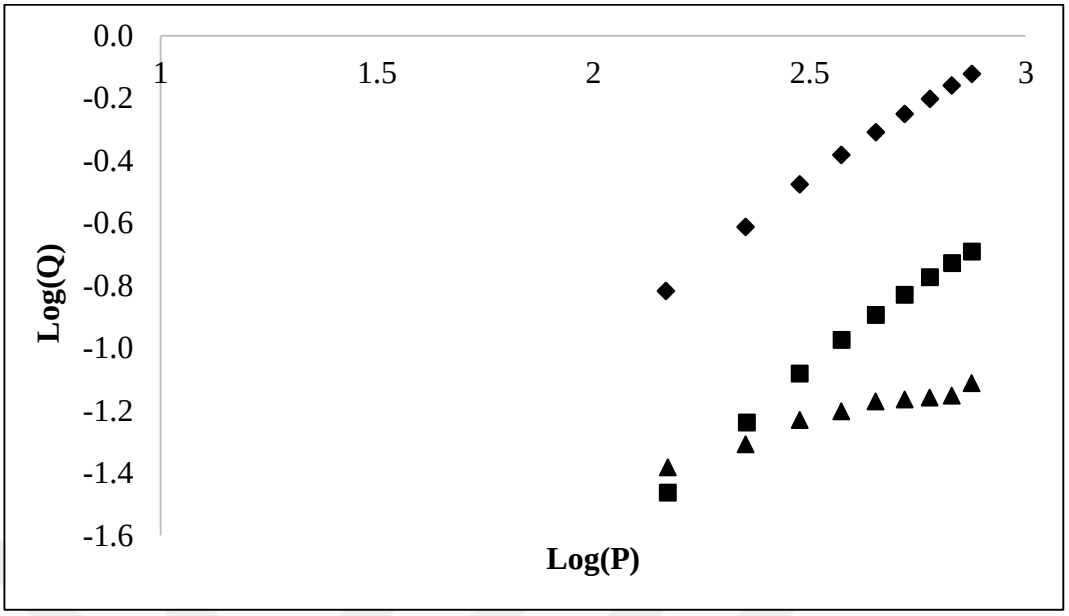

Figure 4.32. Freundlich Isotherms of CH_4 adsorption on A8-250 (♦) 25 °C, (■) 120 °C and (▲) 200 °C.

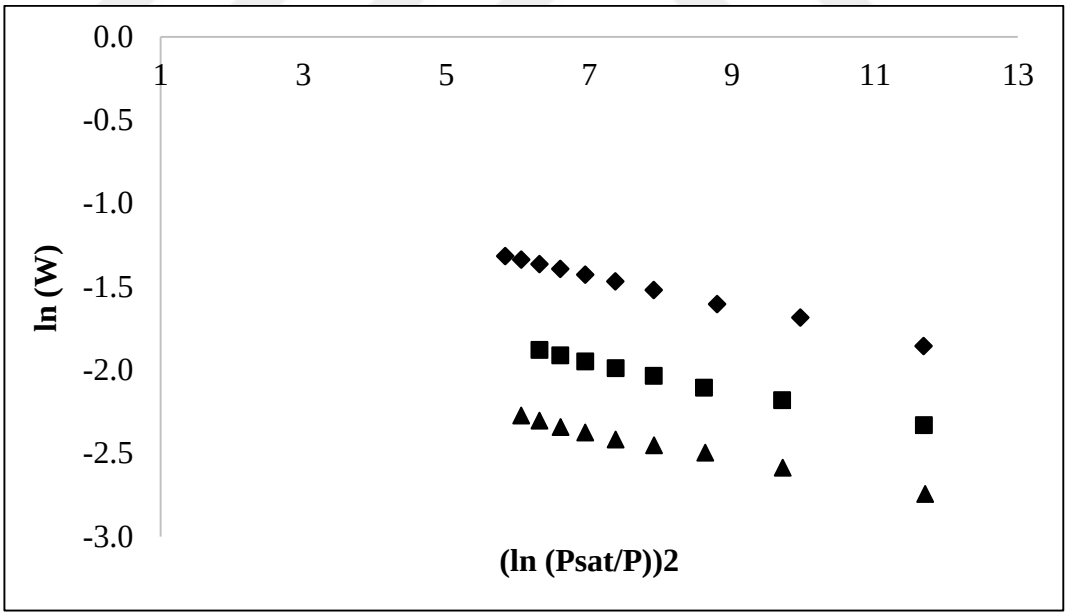

Figure 4.33. D-R Isotherms of CO_2 adsorption on A8-250 (♦) 25 °C, (■) 120 °C and (▲) 200 °C.

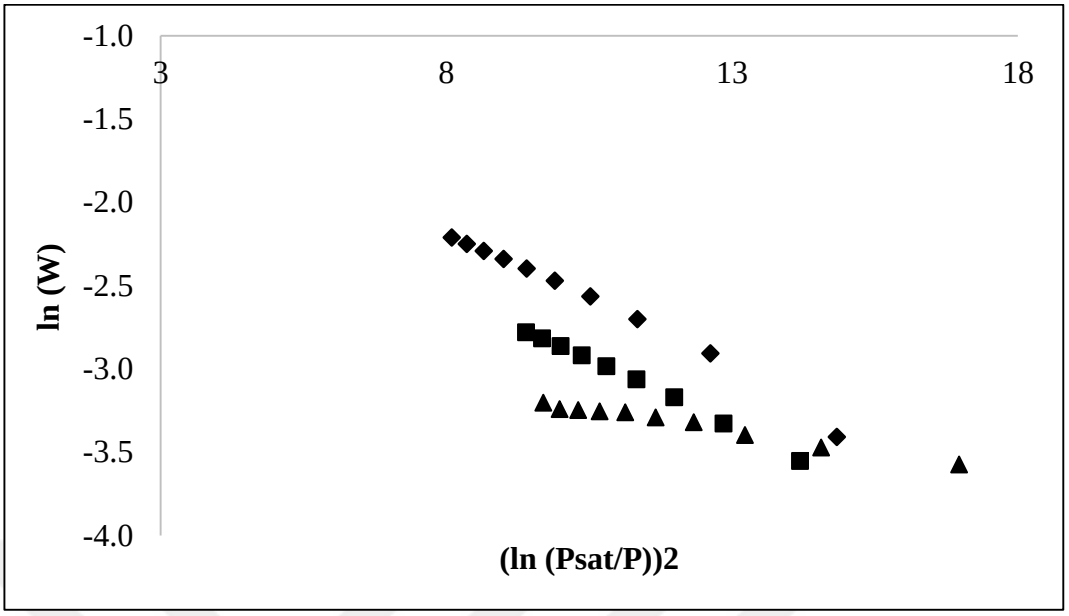

Figure 4.34. D-R Isotherms of CH_4 adsorption on A8-250 (♦) 25 °C, (■) 120 °C and (▲) 200 °C.

Regression analysis indicated that Langmuir adsorption model can only be used for CO_2 adsorption results obtained at RT. As Langmuir model based on the assumption of homogeneity of the surface, the lack of fit is an expected outcome validating SEM results (from section 4.1) showing the heterogeneity of AC samples.

Table 4.1. Langmuir Isotherm parameters for CO_2 adsorption.

Sample	Langmuir constants (25°C)			Langmuir constants (120°C)			Langmuir constants (200°C)		
	Q_m	b	R^2	Q_m	b	R^2	Q_m	b	R^2
AC8-200	0.6323	0.0006	0.9988	2.6610	0.0031	0.9622	0.7342	0.0031	0.9411
AC8-250	3.1786	0.0026	0.9844	1.0927	0.0020	0.9899	0.9242	0.0033	0.9577
AC8-300	3.6536	0.0028	0.9964	2.6144	0.0023	0.9685	0.3760	0.0034	0.9712
AC9-175	6.4103	0.0029	0.9959						
AC9-200	2.1061	0.0044	0.9910	3.2510	0.0005	0.9206			
AC9-250	2.0812	0.0030	0.9950						

Table 4.2. Langmuir Isotherm parameters for CH_4 adsorption.

Sample	Langmuir constants (25°C)			Langmuir constants (120°C)			Langmuir constants (200°C)		
	Q_m	b	R^2	Q_m	b	R^2	Q_m	b	R^2
AC8-200	2.3447	0.0009	0.9963	0.1631	0.0031	0.9757	0.0183	0.0086	0.8905
AC8-250	2.1519	0.0002	0.8186	1.2384	0.0002	0.4008	0.0935	0.0053	0.9877
AC8-300	0.4065	0.0006	0.5079	0.2840	0.0009	0.9992	0.0386	0.0291	0.9454
AC9-175	0.5492	0.0006	0.9860						
AC9-200	0.6342	0.0006	0.9979	0.0796	0.0015	0.8174			
AC9-250	0.6323	0.0006	0.9988						

Freundlih model parameters, k and 1/n, for CO_2 adsorption are given at Table 4.6. All parameters were calculated from log(Q) vs. log(P) graphs. The Freundlich isotherm assumes a heterogeneous surface (multilayer adsorption) with a non-uniform distribution of heat of adsorption over it [54]. The decrease in the values of k at higher temperatures shows that the adsorption rate decreases with increasing temperature. Only for AC8-300 sample, k value calculated at 200 °C was higher than k value calculated at 120 °C. For all samples, 1/n values were between 0-1 range (Table 4.6). Therefore, Freundlich Isotherm was found to be suitable for modelling CO_2 adsorption on these adsorbents. High 1/n values can be associated with more homogeneous surfaces [54]. While for AC8 samples increasing temperature did not affect 1/n values, significant increase in 1/n value for AC9-200 points out the significant decrease of the surface heterogeneity of AC9-200 at elevated adsorption temperatures.

As it can be seen from Freundlich isotherm parameters obtained based on CH_4 adsorption data (Table 4.7), although correlation coefficient for all samples but AC8-300 were 0.99 at RT, at higher temperatures, especially at 200 °C, correlation coefficient values decreased for Freundlich isotherm parameters. On the other hand, as 1/n parameters calculated are over 1 for many of the adsorbents, Freundlich isotherm was found not suitable for explaining CH_4 adsorption behavior of the samples.

Table 4.3. Freundlich Isotherm parameters for CO_2 adsorption.

Sample	Freundlich constants (25°C)			Freundlich constants (120°C)			Freundlich constants (200°C)		
	k	1/n	R^2	k	1/n	R^2	k	1/n	R^2
AC8-200	0.0934	0.4878	0.9991	0.0271	0.4905	0.9977	0.0052	0.5497	0.9946
AC8-250	0.0658	0.5287	0.9977	0.0195	0.5327	0.9995	0.0102	0.4804	0.9948
AC8-300	0.1172	0.4639	0.9997	0.0129	0.5856	0.9995	0.0198	0.3952	0.9924
AC9-175	0.0864	0.4432	0.9998						
AC9-200	0.0967	0.4324	0.9981	0.0013	0.8295	0.9986			
AC9-250	0.0552	0.4988	0.9971						

Table 4.4. Freundlich Isotherm parameters for CH_4 adsorption.

Sample	Freundlich constants (25°C)			Freundlich constants (120°C)			Freundlich constants (200°C)		
	k	1/n	R^2	k	1/n	R^2	k	1/n	R^2
AC8-200	0.0070	0.7417	0.9988	0.0218	0.4017	0.9863	0.7053	-0.5246	0.6856
AC8-250	0.0012	0.9765	0.9960	0.0002	1.0984	0.9951	0.0072	0.3594	0.9582
AC8-300	0.0001	1.3085	0.9813	0.0022	0.7623	0.9984	0.0042	0.3454	0.6149
AC9-175	0.0010	0.9417	0.9906						
AC9-200	0.0015	0.8963	0.9936	0.0001	1.0695	0.9671			
AC9-250	0.0015	0.8951	0.9937						

D-R model parameters, k and 1/n, for CO_2 adsorption are given in Table 4.8. All parameters were calculated from ln(W) vs. $(\ln(P_{sat}/P))^2$ graphs. The micro pore capacity (W_0) and characteristic energy values for all adsorbents are listed in Tables 4.8-9. While for all adsorbents CO_2 micro pore capacities decreased with increasing temperature, the calculations showed that air oxidized samples (AC8s) have higher micro pore capacities compared to those of HNO_3 oxidized samples (AC9s). This deduction is in accordance with the experimental adsorption data. While at RT all AC8s have higher micro pore capacities, at 120 °C AC9-200 sample has the highest micro pore capacity. This can be resulting from

the surface change due to decomposition of the carboxylic acid groups from the sample surface at high temperatures. The values below 8 kJ/mol indicate physical adsorption whereas characteristic energies above that value till 16 kJ/mol points to ion exchange [54]. Therefore we can conclude that physisorption is not the only CO_2 adsorption mechanism for all the adsorbents studied at RT; ion exchange mechanism may also play an additional role.

Table 4.5. D-R Isotherm parameters for CO_2 adsorption.

Sample	D-R constants (25°C)			D-R constants (120°C)			D-R constants (200°C)		
	Wo (cc/g)	E (J/mol)	R^2	Wo (cc/g)	E (J/mol)	R^2	Wo (cc/g)	E (J/mol)	R^2
AC8-200	0.1655	8.3335	0.9988	0.0473	8.5284	0.9915	0.0179	7.6434	0.9921
AC8-250	0.1616	8.2047	0.9982	0.0453	8.4439	0.9926	0.0163	8.6575	0.9903
AC8-300	0.1618	8.7650	0.9988	0.0526	7.8008	0.9979	0.0211	8.2182	0.9907
AC9-175	0.1086	8.6469	0.9998						
AC9-200	0.1012	9.0646	0.9999	0.0869	6.7649	0.9984			
AC9-250	0.1512	9.3435	0.9999						

Table 4.6. D-R Isotherm parameters for CH_4 adsorption.

Sample	D-R constants (25°C)			D-R constants (120°C)			D-R constants (200°C)		
	Wo (cc/g)	E (J/mol)	R^2	Wo (cc/g)	E (J/mol)	R^2	Wo (cc/g)	E (J/mol)	R^2
AC8-200	0.0597	7.4277	0.9977	0.0124	9.2391	0.9963	0.0000	8.8995	0.9397
AC8-250	0.1654	5.9673	0.9902	0.0566	6.1689	0.9983	0.0020	10.9563	0.9841
AC8-300	0.2994	5.4608	0.9889	0.0272	7.5612	0.9995	0.0020	9.0046	0.8371
AC9-175	0.0577	6.5766	0.9958						
AC9-200	0.0550	6.7448	0.9987	0.0284	6.3735	0.9735			
AC9-250	0.0548	6.7498	0.9988						

While CH_4 adsorption data studied with D-R model, only the parameters with correlation coefficient of ca. 0.99 were considered. All AC9 adsorbents and AC8-200 adsorbent had very low and similar micro pore capacities (~0.055-0.060) for CH_4 adsorption.

Characteristic energy values from Table 4.9 indicated that physisorption is the only CH_4 adsorption mechanism for all the adsorbents studied at RT.

4.3.2. Adsorption Kinetics

The data used for kinetic modelling of CO_2 and CH_4 adsorption on AC8 adsorbents are given in Figures 4.35 and 4.36, respectively. Pseudo-first order and pseudo-second order kinetic models were fitted to kinetic data (Figure 4.37-39). The parameters obtained from the application of pseudo-first and pseudo-second order kinetic models to these kinetic data yielding R^2 values higher than 0.99 are given in Tables 10 and 11, respectively. The results show that while pseudo-first order kinetic model successfully explained both CO_2 and CH_4 adsorption kinetics at RT, CH_4 adsorption kinetics on AC8-200 and AC8-300 adsorbents were more suitably explained by pseudo-second order kinetic model.

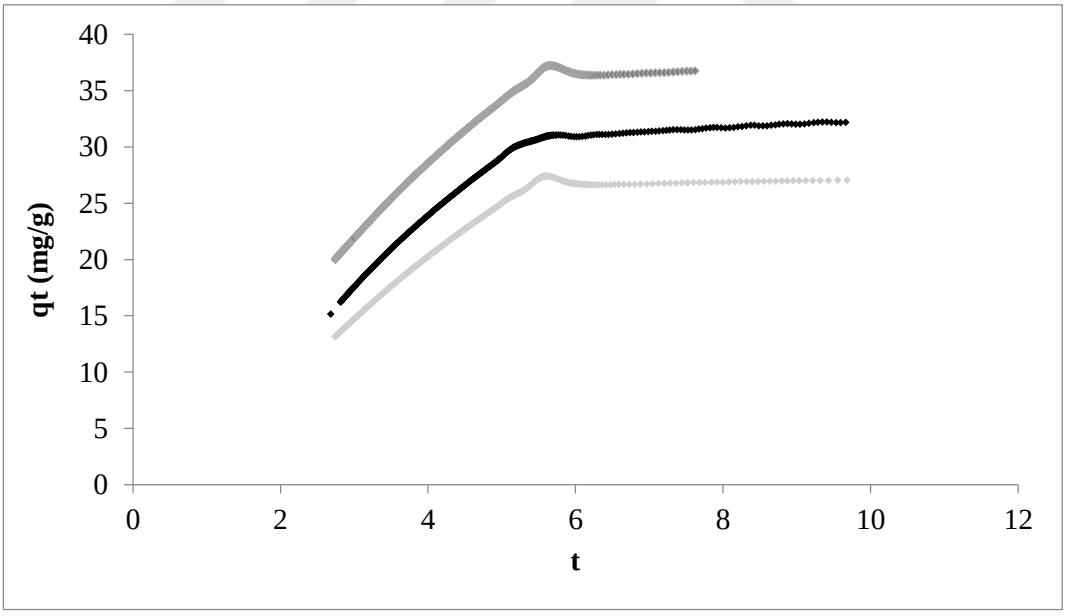

Figure 4.35. Kinetic graphs for CO_2 adsorption at RT: (▉) AC8-200, (-) AC8-250, (-) AC8-300.

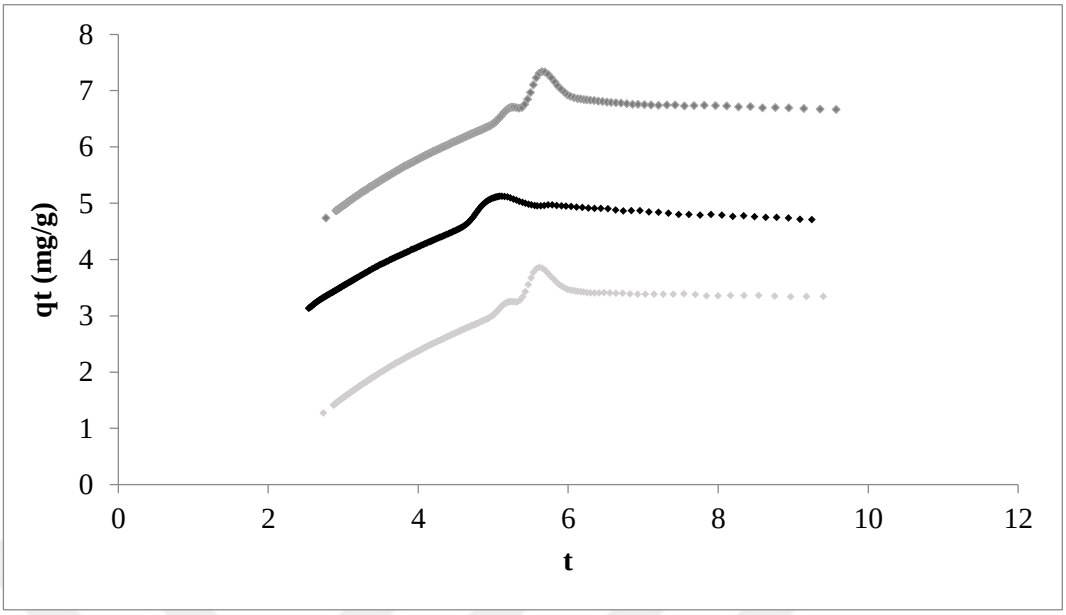

Figure 4.36. Kinetic graphs for CH_4 adsorption at RT: (▉) AC8-200, (-) AC8-250, (-) AC8-300.

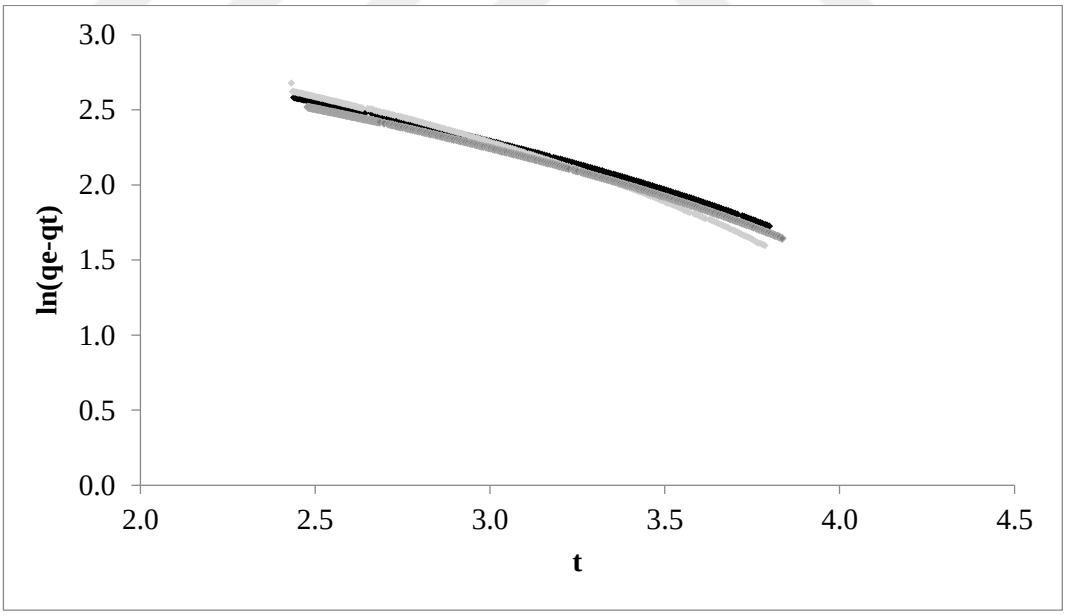

Figure 4.37. Pseudo-first order kinetic models for CO_2 adsorption at RT: (▉) AC8-200, (-) AC8-250, (-) AC8-300.

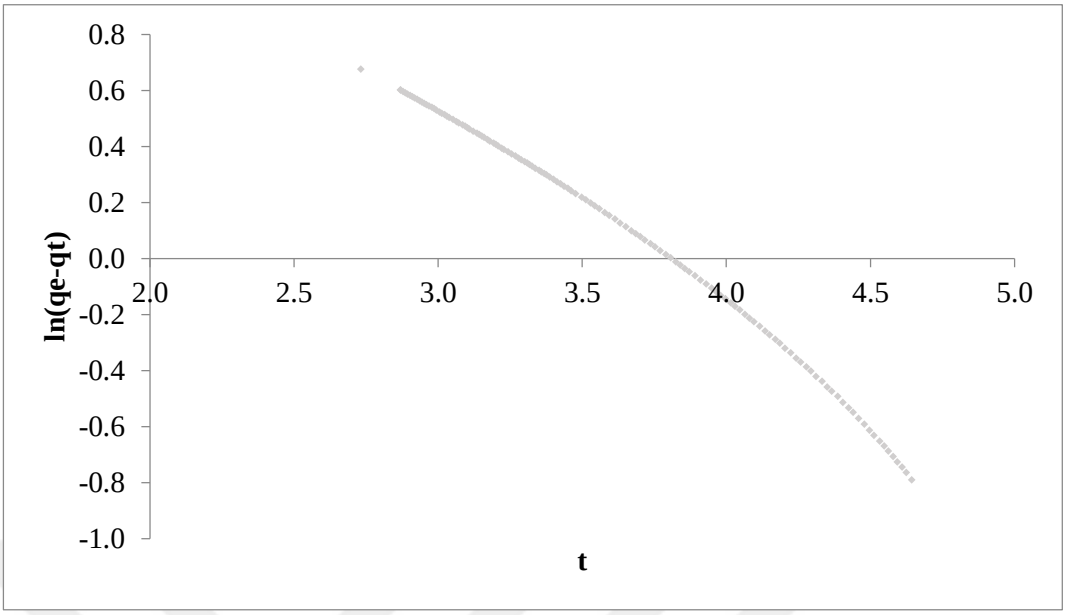

Figure 4.38. Pseudo-first order kinetic model for CH_4 adsorption at RT: (-) AC8-250.

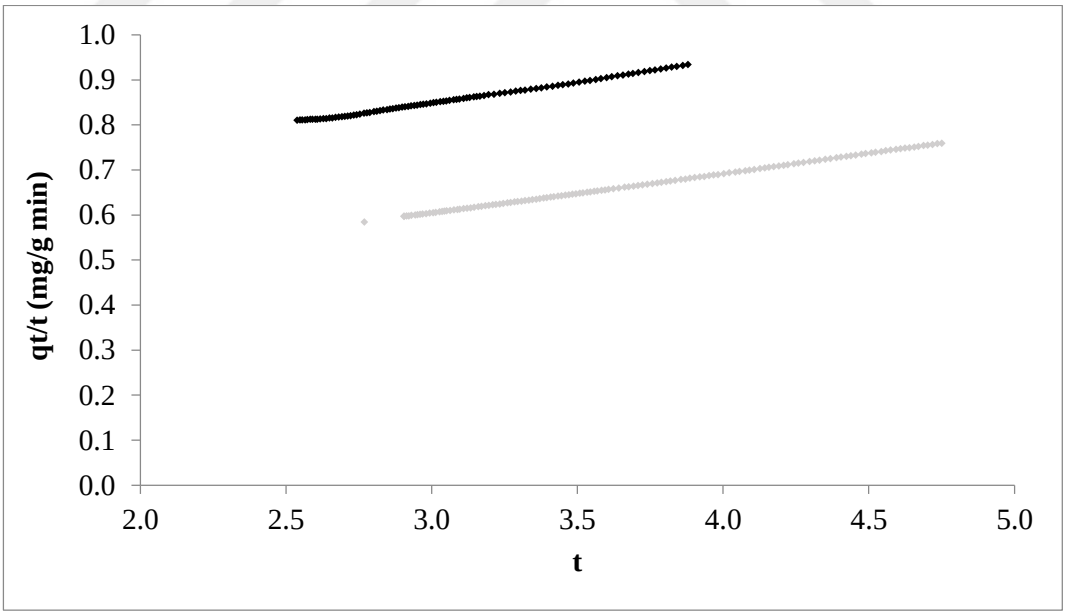

Figure 4.39. Pseudo-second order kinetic models for CH_4 adsorption at RT: (■) AC8-200, (-) AC8-300.

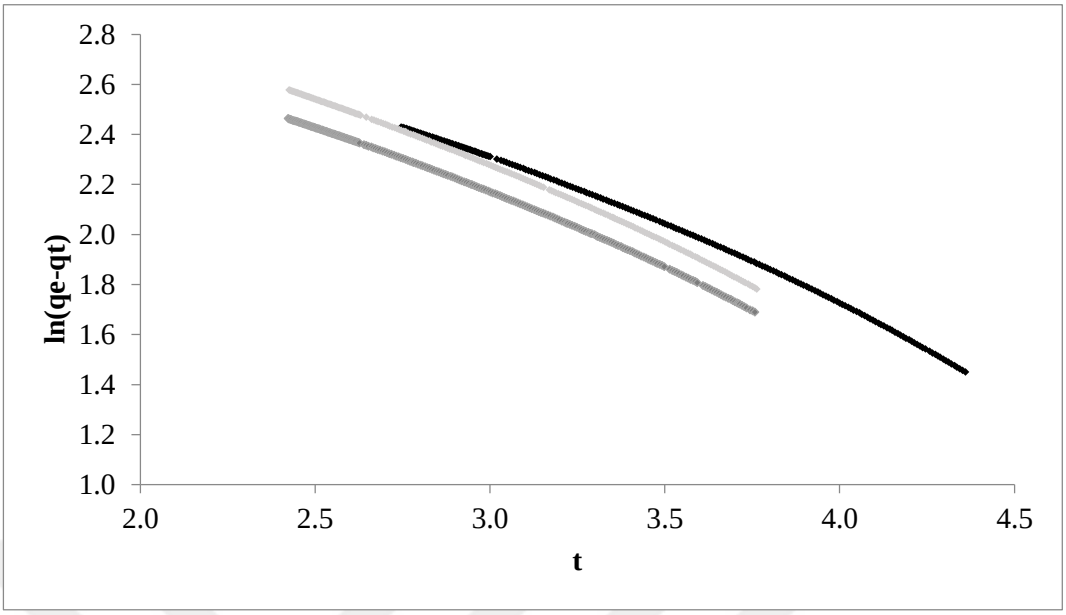

Figure 4.40. Pseudo-first order kinetic models for CO_2 adsorption at RT: (▉) AC9-175, (▉) AC9-200, (▉) AC9-250.

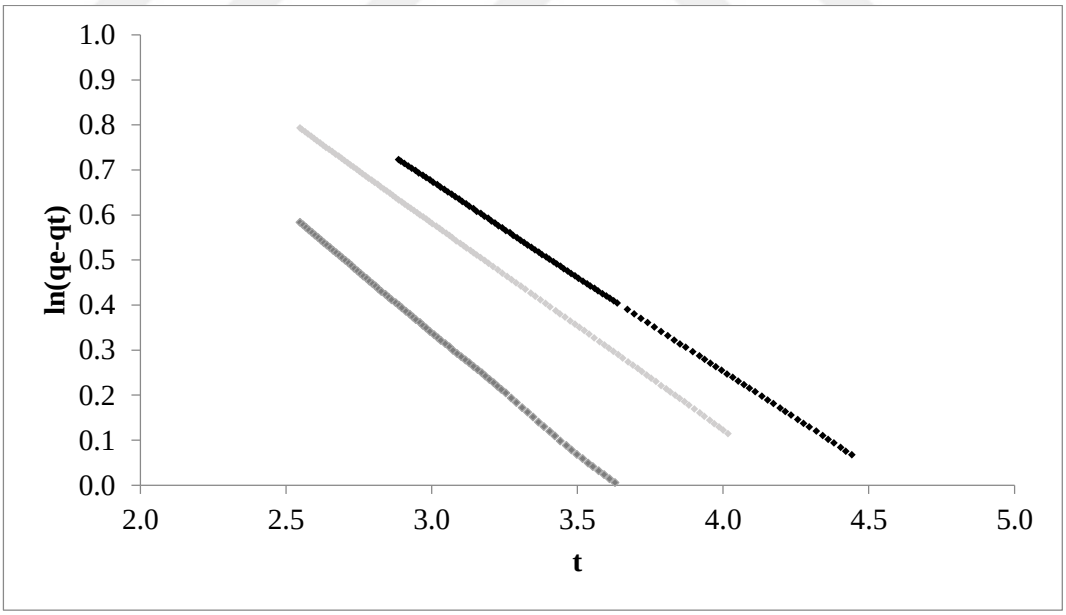

Figure 4.41. Pseudo-first order kinetic models for CH_4 adsorption at RT: (▉) AC9-175, (▉) AC9-200, (▉) AC9-250.

Table 4.7. Pseudo-first order kinetic model parameters for CO_2 and CH_4 adsorptions at RT.

	CO_2			CH_4		
Adsorbent	k_1 (min^{-1})	q_e (mg/g)	R^2	k_1 (min^{-1})	q_e (mg/g)	R^2
AC8-200	0.5844	80.3346	0.9954			
AC8-250	0.6144	76.9688	0.9911	0.7437	16.2209	0.9903
AC8-300	0.5679	82.7646	0.9949			
AC9-175	0.5918	59.6921	0.9943	0.6380	46.8664	0.9917
AC9-200	0.5833	55.3070	0.9969	0.7389	56.2272	0.9920
AC9-250	0.5686	47.5461	0.9966	0.5553	7.4358	0.9990

Table 4.8. Pseudo-second order kinetic model parameters for CH_4 adsorption at RT.

	CH_4		
Adsorbent	k_2 ($gmg^{-1}min^{-1}$)	q_e (mg/g)	R^2
AC8-200	0.0169	10.3093	0.9990
AC8-300	0.0231	11.3122	0.9998

5. CONCLUSIONS AND RECOMMENDATIONS

5.1. Conclusions

Air oxidized and K_2CO_3 impregnated samples belong to AC8 set, and HNO_3 oxidized and K_2CO_3 impregnated samples belong to AC9 set; were prepared through high temperature heat treatment, oxidation, and K_2CO_3 impregnation followed by calcination at different temperature levels (i.e. 200 °C, 250 °C and 300 °C for AC8s, 175 °C, 200 °C and 250 °C for AC8s). All samples were characterized by SEM-EDX; and tested for their adsorption/selective adsorption performances at both 0-1000 mbar and at 0-5000 mbar (total) pressure range by using IGA-DSMS system. The major conclusions that can be drawn from current study can be summarized as follows:

- The SEM images revealed that clusters formed on AC8s are not homogeneously distributed over the adsorbent, while AC9 adsorbents seemed to have similar surfaces on which K-formations homogeneously dispersed with smaller size. EDX results in general confirmed surfaces of AC8 samples have 5-7% K^+ on the average, whereas AC9 samples had 8-9% K^+ average surface concentration. The results also show that on AC8 surfaces the exposed amount of K^+% increased with the increase in calcination temperature applied during the preparation of the adsorbent, while the calcination temperature did not significantly affect K^+ surface concentration of AC9 series adsorbents.

- The adsorption/desorption tests conducted at three different temperatures i.e. RT, 120 °C and 200 °C, showed that adsorbed amount of both CO_2 and CH_4 decreases with the increase in temperature. In desorption process, temperature was led to a just the opposite trend; at high temperature, desorption occurred more easily than it did at RT.

- In the pure gas tests, the CO_2 mass uptake capacities of the designed and prepared samples at RT and 1000 mbar were 7-8 times higher than their CH_4 mass uptake capacities at the same conditions.

- When the effect of oxidation type investigated, the adsorption/selective adsorption performance of HNO_3 oxidized AC9 series adsorbents, were found inferior compared to the performance of the AC8 series adsorbents.

- Comparing the adsorption isotherms of the samples with different calcination temperatures showed that the higher the calcination temperature, the more stable the surfaces become.

- At 1000 mbar and RT, the highest pure CO_2 adsorption capacity was observed for AC8-300 sample, while it exhibited similar CH_4 adsorption capacity to AC8-200. CO_2 adsorption is confirmed to be reversible on all samples as there is no significant deviation observed between their adsorption and desorption profiles, whereas partial irreversibility was observed for CH_4 adsorption.

- AC8-200 has the highest mass based CO_2:CH_4 adsorption selectivity ratio for the 50% CO_2-50% CH_4 feed gas mixture, whereas AC8-250 reached the highest CO_2:CH_4 selectivity ratio for 10% CO_2-90% CH_4 feed gas mixture.

- The CO_2 adsorption on the AC8-200 sample was 19.7 wt.% at 5000 mbar. As for 50% CO_2-50% CH_4 feed gas mixture, the mass based adsorption selectivity ratio CO_2:CH_4 on AC8-200 is 3.8 at RT for 0-5000 mbar total pressure, the mass based adsorption selectivity ratio for the tests conducted with 10% CO_2-90% CH_4 feed gas mixture was calculated as 0.5. In response to the decrease in CO_2:CH_4 feed ratio from 2.75 to 0.3, the adsorption selectivity ratio decreases from 3.89 to 0.5.

- A clear match between mass uptake trends obtained for pure gas feeds in 0-1000 mbar and 0-5000 mbar pressure ranges showed the reliability of the adsorption measurements.

The experimental adsorption isotherm data, which were obtained for three temperature values, i.e. RT, 120 °C and 200 °C, between 0-1000 mbar pressure range were fitted to Langmuir, Freundlich and Dubinin-Radushkevich (D-R) models to describe the adsorption

characteristics of the designed and prepared adsorbents. Pseudo-first order and pseudo-second order kinetic models were fitted to kinetic data.

- According to correlation analysis results, Freundlich and D-R models were found more successful in explaining CO_2 and CH_4 adsorption behaviors of AC samples. As it was expected, Langmuir isotherm model which is based on the monolayer adsorption assumption was not good at explaining the adsorption behaviors of ACs.

- While pseudo-first order kinetic model successfully explained both CO_2 and CH_4 adsorption kinetics at RT, CH_4 adsorption kinetics on AC8-200 and AC8-300 adsorbents were more suitably explained by pseudo-second order kinetic model.

5.2. Recommendations

Considering the results of the experimental study, following ideas are thought to be beneficial for future studies:

- Different K_2CO_3 loadings can be studied to find the optimum loading.

- The ‘modified AC based adsorbents’ can be impregnated with different alkali promoters, so that the effect of different alkali impregnations to CO_2 adsorption capacity and selective adsorption performance can be compared.

- As the adsorption/selective adsorption performance of the samples prepared on HNO_3 oxidized AC support were found inferior compared to the performance of the samples prepared on air oxidized AC support; the effect of air oxidation can be further studied in detail through the preparation, characterization and testing of new AC-based adsorbent samples prepared on the supports for which the air (gas phase) oxidation is performed by using N_2+O_2 mixtures having different mixture composition.

- Water can be connected to IGA-DSMS system in order to observe the adsorption/selective adsorption performance of the AC-based samples in the presence of moisture.

- High pressure adsorption tests can be conducted under elevated temperatures, so that effect of temperature can be further investigated.

- In order to describe the selective adsorption characteristics of the designed and prepared adsorbents, kinetic data from selective adsorption tests can be modified to be fitted kinetic models.

REFERENCES

1. Intergovernmental Panel on Climate Change, "Summary for Policymakers. In Climate Change 2007: The Physical Science Basis, Contribution of Working Group I to the Fourth Assessment Report of the Intergovernmental Panel on Climate Change*", Geneva: World Meteorological Organization/United Nations Environment Program,* 2007.

2. Yang, H. , Z. Xu , M. Fan, R. Gupta , R.B. Slimane , A.E. Bland, and I. Wright , "Progress in Carbon Dioxide Separation and Capture: A Review", *Journal of Environmental Sciences* , Vol. 20, pp. 14-27, 2008.

3. Bandyopadhyay, A., "Amine versus Ammonia Absorption of CO_2 as a Measure of Reducing GHG Emission: A Critical Analysis". *Clean Technologies and Environmental Policy*, Vol. 13, pp. 269-294, 2011.

4. Mondal, M.K., H.K. Balsora, and P. Varshney, "Progress and Trends in CO_2 Capture/Separation Technologies: A Review", *Energy*, Vol. 46, pp. 43-441, 2012.

5. Pires, J.C.M., F.G. Martins, M.C.M. Alvim-Ferraz, and M. Simões, "Recent Developments on Carbon Capture and Storage: An Overview", *Chemical Engineering Research and Design*, Vol. 89, pp. 1446-1460, 2011.

6. Thiruvenkatachari, R., S. Su, H. An, and X.X. Yu, "Post Combustion CO_2 Capture by Carbon Fibre Monolithic Adsorbents", *Progress in Energy and Combustion Science*, Vol. 35, pp. 438-455, 2009.

7. Kanniche, M., R. Gros-Bonnivard, P. Jaud, J. Valle-Marcos, J.M. Amann, and C. Bouallou, "Pre-combustion, Post-combustion and Oxy-combustion in Thermal Power Plant for CO_2 Capture", *Applied Thermal Engineering* , Vol. 30, pp. 53-62, 2010.

8. Caglayan, B.S., and A.E. Aksoylu, "CO_2 Adsorption on Chemically Modified Activated Carbon", *Journal of Hazardous Materials*, Vol. 252– 253, pp. 19-28, 2013.

9. Rufford, T.E., S. Smart, G.C.Y. Watson, B.F. Graham, J. Boxall, J.C. Costa, and E.F. May, "The Removal of CO_2 and N_2 from Natural Gas: A Review of Conventional and Emerging Process Technologies", *Journal of Petroleum Science and Engineering*, Vol. 94-95,pp. 123-154, 2012.

10. Sayari, A., Y. Belmabkhout, and R. Serna-Guerrero, "Flue Gas Treatment via CO_2 Adsorption", *Chemical Engineering Journal*, Vol. 171, pp. 760-774, 2011.

11. Wang, D., C. Sentorun-Shalaby, X. Ma, and C. Song, "High-Capacity and Low-Cost Carbon-Based "Molecular Basket" Sorbent for CO_2 Capture from Flue Gas", *Energy Fuels*, Vol. 25, pp. 456-458, 2010.

12. Jadhav, P.D., R.V. Chatti, R.B. Biniwale, N.K. Labhsetwar, S. Devotta, and S.S. Rayalu, "Monoethanol Amine Modified Zeolite 13X for CO_2 Adsorption at Different Temperatures", *Energy & Fuels*, Vol. 21, pp. 3555-3559, 2007.

13. Plaza, M.G., C. Pevida, B. Arias, M.D. Casai, C.F. Martin, J. Fermoso, F. Rubiera, and J.J. Pis, "Different Approaches for the Development of Low Cost CO_2 Adsorbents", *Journal of Environmental Engineering*, Vol. 135, pp. 426-431, 2009.

14. Yu, C.H., C.H. Huang, and C.S. Tan, "A Review of CO_2 Capture by Absorption and Adsorption", *Aerosol and Air Quality Research*, Vol. 12, pp.745-769, 2012.

15. Thang, H.V., L. Grajciar, P. Nachtigall, O. Bludsk´y, C.O. Areán, E. Frydova, and R. Bulánek, "Adsorption of CO_2 in FAU Zeolites: Effect of Zeolite Composition", *Catalysis Today*, Vol. 227, pp. 50-56, 2013.

16. Maurin, G., P.L. Llewellyn, and R.G. Bell, "Adsorption Mechanism of Carbon Dioxide in Faujasites: Grand Canonical Monte Carlo Simulations and Microcalorimetry Measurements", *The Journal of Physical Chemistry B*, Vol. 109, pp. 16084-16091, 2005.

17. Walton, K.S., M.B. Abney, and M.D. LeVan, "CO_2 Adsorption in Y and X Zeolites Modified by Alkali Metal Cation Exchange", *Microporous and Mesoporous Materials*, Vol. 91, pp. 78-84, 2006.

18. Zukal, A., J. Pawlesa, and J. Cejka, "Isosteric Heats of Adsorption of Carbon Dioxide on Zeolite MCM-22 Modified by Alkali Metal Cations", *Adsorption*, Vol. 15, pp. 264-270, 2009.

19. Chen, C., D.W. Park, and W.S. Ahn, "CO_2 Capture Using Zeolite 13X Prepared from Bentonite", *Applied Surface Science*, Vol. 292, pp. 63-67, 2014.

20. Jiang, Q., J. Rentschler, G. Sethia, S. Weinman, R. Perrone, and K. Liu, "Synthesis of T-type Zeolite Nanoparticles for the Separation of CO_2/N_2 and CO_2/CH_4 by Adsorption Process", *Chemical Engineering Journal*, Vol. 230, pp. 380-388, 2013.

21. Deroche, I., L. Gaberova, G. Maurin, P.L. Llewellyn, M. Castro, and P. Wright, "Adsorption of Carbon Dioxide in SAPO STA-7 and Alpo-18: Grand Canonical Monte Carlo Simulations and Microcalorimetry Measurements", *Adsorption*, Vol. 14, pp. 207-213, 2008.

22. Castro, M., S.J. Warrender, P. Wright, D.C. Apperley, Y. Belmabkhout, G. Pirngruber, H.K. Min, M.B. Park, and S.B. Hong, "Silicoaluminophosphate Molecular Sieves STA-7 and STA-14 and Their Structure-Dependent Catalytic Performance in the Conversion of Methanol to Olefins", *Journal of Physical Chemistry C*, Vol.113, pp. 15731-15741, 2009.

23. Rowsell, J.L.C., and O.M. Yaghi, "Metal–Organic Frameworks: A New Class of Porous Materials", *Microporous and Mesoporous Materials*, Vol. 73, pp. 3-14, 2004.

24. Millward, A.R., and O.M. Yaghi, "Metal−Organic Frameworks with Exceptionally High Capacity for Storage of Carbon Dioxide at Room Temperature", *Journal of the American Chemical Society*, Vol. 127, pp. 17998-17999, 2005.

25. Caskey, S.R., A.G. Wong-Foy, and A.J. Matzger, "Dramatic Tuning of Carbon Dioxide Uptake via Metal Substitution in a Coordination Polymer with Cylindrical Pores", *Journal of the American Chemical Society*, Vol. 130, pp. 10870-10871, 2008.

26. Barcia, P.S., L. Bastin, E.J. Hurtado, J.A.C. Silva, A.E. Rodrigues, and B. Chen, "Single and Multicomponent Sorption of CO_2, CH_4 and N_2 in a Microporous Metal-Organic Framework", *Separation Science and Technology*, Vol. 43, pp. 3494-3521, 2008.

27. Li, Y., and R.T. Yang, "Gas Adsorption and Storage in Metal-Organic Framework MOF- 177", *Langmuir*, Vol. 23, pp. 12937-12944, 2007.

28. Park, K.S., Z. Ni, A.P. Côté, R. Choi, R. Huang, F.J. Unribe-Romo, H.K. Chae, M. O'Keeffe, and O.M. Yaghi, "Exceptional Chemical and Thermal Stability of Zeolitic Imidazolate Frameworks", *Proceedings of the National Academy of Sciences*, Vol. 103, pp. 10186-10191,2006.

29. Phan, A., C.J. Doonan, F.J. Urıbe-Romo, C.B. Knobler, M. O'Keeffe, and O.M. Yaghı, "Synthesis, Structure, and Carbon Dioxide Capture Properties of Zeolitic Imidazolate Frameworks", *Accounts Of Chemical Research*, Vol. 43, pp. 58-67, 2010.

30. Furukawa, H., and O.M. Yaghi, "Storage of Hydrogen, Methane, and Carbon Dioxide in Highly Porous Covalent Organic Frameworks for Clean Energy Applications", *Journal of the American Chemical Society*, Vol. 131, pp. 8875-8883, 2009.

31. Wahby, A., J. Silvestre-Albero, A. Sepúlveda-Escribano, and F. Rodríguez-Reinoso, "CO_2 Adsorption on Carbon Molecular Sieves", *Microporous and Mesoporous Materials*, Vol. 164, pp. 280-287, 2012.

32. Huang, L., L. Zhang, Q. Shao, L. Lu, X. Lu, S. Jiang, and W. Shen, "Simulations of Binary Mixture Adsorption of Carbon Dioxide and Methane in Carbon Nanotubes: Temperature, Pressure, and Pore Size Effects", *Journal of Physical Chemistry C*, Vol. 111, pp. 11912-11920, 2007.

33. Yin, G., Z. Liu, Q. Liu, and W. Wu, "The Role of Different Properties of Activated Carbon in CO_2 Adsorption", *Chemical Engineering Journal*, Vol. 230, pp.133-140, 2013.

34. Lee, S.Y., and S.J. Park, "A Review on Solid Adsorbents for Carbon Dioxide Capture", *Journal of Industrial and Engineering Chemistry*, Vol. 23, pp. 1-11, 2015.

35. Shahkarami, S., R. Azargohar, A.K. Dalai, and J. Soltan, "Breakthrough CO_2 Adsorption in Bio-Based Activated Carbons", *Journal of Environmental Sciences*, Vol. 34, pp. 68-76, 2015.

36. Lee, S.Y., and S.J. Park, "Determination of the Optimal Pore Size for Improved CO_2 Adsorption in Activated Carbon Fibers", *Journal of Colloid and Interface Science,* Vol. 389, pp. 230-235, 2013.

37. Shafeeyan, M.S., W.M.A.W. Daud, A. Houshmand, and A. Shamiri, "A Review on Surface Modification of Activated Carbon for Carbon Dioxide Adsorption", *Journal of Analytical and Applied Pyrolysis*, Vol. 89, pp. 143-151, 2010.

38. Shafeeyan, M.S., W.M.A.W Daud, A. Houshmand, and A. Arami-Niya, "Ammonia Modification of Activated Carbon to Enhance Carbon Dioxide Adsorption: Effect of Pre-Oxidation", *Applied Surface Science*, Vol. 257, pp. 3936-3942, 2011.

39. Heidari, A., H. Younesi, A. Rashidi, and A.A. Ghoreyshi, "Evaluation of CO_2 Adsorption with Eucalyptus Wood Based Activated Carbon Modified by Ammonia Solution through Heat Treatment", *Chemical Engineering Journal*, Vol. 254, pp. 503-513, 2014.

40. Lee, C.S., Y.L. Ong, M.K. Aroua, and W.M.A.W. Daud, "Impregnation of Palm Shell-Based Activated Carbon with Sterically Hindered Amines for CO_2 Adsorption", *Chemical Engineering Journal*, Vol. 219, pp. 558-564, 2013.

41. Zhang, Z., M. Xu, H. Wang, and Z. Li, "Enhancement of CO_2 Adsorption on High Surface Area Activated Carbon Modified by N_2, H_2 and NH_3", *Chemical Engineering Journal*, Vol. 160, pp. 571-577, 2010.

42. Somy, A., M.R. Mehrnia, H.D. Amrei, A. Ghanizadeh, and M. Safari, "Adsorption of Carbon Dioxide using Impregnated Activated Carbon Promoted by Zinc", *International Journal of Greenhouse Gas Control*, Vol. 3, pp. 249-254, 2009.

43. Guo, Y., C. Zhao, C. Li, and S. Lu, "Application of PEI–K_2CO_3/AC for Capturing CO_2 from Flue Gas after Combustion", *Applied Energy*, Vol. 129, pp. 17-24, 2014.

44. Arami-Niya, A., W.M.A.W. Daud, F.S. Mjalli, F. Abnisa, and M.S. Shafeeyan, "Production of Microporous Palm Shell Based Activated Carbon for Methane Adsorption: Modeling and Optimization Using Response Surface Methodology", *Chemical Engineering Research And Design*, Vol. 90, pp. 776-784, 2012.

45. Yang, H., M. Gong, and Y. Chen, "Preparation of Activated Carbons and Their Adsorption Properties for Greenhouse Gases: CH_4 and CO_2", *Journal of Natural Gas Chemistry*, Vol. 20, pp. 460-464, 2011.

46. Grande, C.A., R. Blom, A. Möller, and J. Möllmer, "High-Pressure Separation of CH_4/CO_2 Using Activated Carbon", *Chemical Engineering Science*, Vol. 89, pp. 10-20, 2013.

47. Gil, M.V., N. Álvarez-Gutiérrez, M. Martínez, F. Rubiera, C. Pevida, A. Morán, "Carbon Adsorbents for CO_2 Capture from Bio-Hydrogen and Biogas Streams: Breakthrough Adsorption Study", *Chemical Engineering Journal*, Vol. 269, pp. 148-158, 2015.

48. Mason, J.A., T.M. McDonald, T.H. Bae, J.E. Bachman, K. Sumida, J.J. Dutton, S.S. Kaye, and J.R. Long, "Application of a High-Throughput Analyzer in Evaluating Solid Adsorbents for Post-Combustion Carbon Capture via Multicomponent Adsorption of

CO_2, N_2, and H_2O", *Journal of the American Chemical Society*, Vol. 137, pp. 4787-4803, 2015.

49. Yi, H., F. Li, P. Ning, X. Tang, J. Peng, Y. Li, and H. Deng, "Adsorption Separation of CO_2, CH_4, and N_2 on Microwave Activated Carbon", *Chemical Engineering Journal*, Vol. 215-216, pp. 635-642, 2013.

50. Hao, W., E. Björkman, M. Lilliestråle, and N. Hedin, "Activated Carbons Prepared from Hydrothermally Carbonized Waste Biomass Used as Adsorbents for CO_2", *Applied Energy*, Vol. 112, pp. 526-532, 2013.

51. Lopes, F.V.S., C.A. Grande, A.M. Ribeiro, J.M. Loureiro, O. Evaggelos, V. Nikolakis, and A.E. Rodrigues, "Adsorption of H_2, CO_2, CH_4, CO, N_2 and H_2O in Activated Carbon and Zeolite for Hydrogen Production", *Sep. Sci. Technol.* , Vol. 44, pp. 1045-1073, 2009.

52. Guo, Y., C. Zhao, C. Li, "CO_2 Adsorption Kinetics of K_2CO_3/Activated Carbon for Low-Concentration CO_2 Removal from Confined Spaces", *Chemical Engineering Technology*, Vol. 38-5, pp. 891-899, 2015.

53. Foo, K.Y., and B.H. Hameed, "Insights into the Modeling of Adsorption Isotherm Systems", *Chemical Engineering Journal*, Vol. 156, pp. 2-10, 2010.

54. Tabatabai, M.A., and D.L. Sparks, *Chemical Processes in Soils*, Soil Science Society of America, Inc., Madison, 2005.

55. Robati, D.,"Pseudo-second Order Kinetic Equations for Modeling Adsorption Systems for Removal of Lead Ions Using Multi-Walled Carbon Nanotube", *Journal Of Nanostructure in Chemistry*, Vol. 3, pp. 1-6, 2013.